DIPLOMARBEIT

Complex Scaling Profiles for Wave Equations in Open Systems

zur Erlangung des akademischen Grades

Diplom-Ingenieurin

im Rahmen des Studiums

Technische Mathematik

durch

Karoline Tichy, BSc.
Matrikelnummer: 01326070

ausgeführt am **Institut für Analysis und Scientific Computing der Technischen Universität Wien**

Betreuung durch

Associate Prof. Dipl.-Math. Dr.rer.nat. Lothar Nannen

Wien, am 9. September 2019 _____ _____

(Unterschrift Verfasserin) (Unterschrift Betreuer)

Kurzfassung

Simulationen offener Ränder sind bei der Betrachtung von Wellenphänomenen von besonderem Interesse. Methoden, welche komplexe Koordinaten-Streckungen verwenden, können angewendet werden, um exponentiell abfallende, auslaufende Lösungen für zeit-harmonische Gleichungen zu generieren. Das Anwenden einer Fourier-Transformation auf das daraus resultierende System im Raum führt zu einem zeitabhängigen System, welches mithilfe der Finite Elemente Methode und passender Zeitschritt-Verfahren diskretisiert werden kann. In dieser Arbeit betrachten wir verschiedene Varianten komplexer Skalierungen für die Wellengleichung und die Klein-Gordon-Gleichung. Wir untersuchen den Effekt von unterschiedlichen Koordinatensystemen und Skalierungs-Funktionen und zeigen ein- und zweidimensionale numerische Ergebnisse.

Abstract

Open boundary simulations are the subject of great interest when considering wave phenomena. Methods using complex coordinate stretchings can be employed to generate exponentially decaying outgoing solutions in space for time-harmonic equations. Applying a Fourier transform to the resulting system in space leads to a system in time domain which can be discretized using the Finite Element Method and an appropriate time-stepping. In this thesis we consider different versions of complex scalings for the wave equation and the Klein-Gordon equation. We study the effects of using different coordinate systems and scaling functions and give numerical results in one and two dimensions.

Acknowledgement

Foremost, I would like to express my greatest appreciation to my advisor Prof. Lothar Nannen for the continuous support of my work. He introduced me to the topic of my thesis and helped me with his guidance and insightful comments whenever needed. I have greatly benefited from him as a professor and mentor.

Besides my advisor, I would like to show my sincere gratitude to Markus Wess for his generous contribution and support.

Furthermore, I want to thank Prof. Joachim Schöberl for providing the necessary infrastructure and resources to accomplish my work.

I am deeply grateful to my family, especially my parents, for supporting me in many ways during my studies. Lastly, I wish to thank Philip for always encouraging me.

Eidesstattliche Erklärung

Ich erkläre an Eides statt, dass ich die vorliegende Diplomarbeit selbstständig und ohne fremde Hilfe verfasst, andere als die angegebenen Quellen und Hilfsmittel nicht benutzt bzw. die wörtlich oder sinngemäß entnommenen Stellen als solche kenntlich gemacht habe.

Wien, am 9. September 2019

Karoline Tichy

Contents

1 Introduction

The aim of this thesis is to discretize wave-type equations in both space and time, and furthermore introduce a complex scaling method to simulate open domains. Within this method we examine the effect of different scalings on the solutions.

The wave problem to be considered in this work is the following: Let $\Omega_{\text{int}} \subset \mathbb{R}^d, d \in \{1,2,3\}$, be a bounded domain, $x \in \mathbb{R}^d$ the spatial variable, and the time interval $[0,T]$ for $T > 0$ with time variable t. We look for a solution $p : \Omega_{\text{int}} \times [0,T] \to \mathbb{R}$ of the wave equation with the following conditions:

$$\frac{1}{c^2}\partial_t^2 p(x,t) = \Delta_x p(x,t), \qquad x \in \Omega_{\text{int}}, t \in [0,T], \tag{1.1}$$

$$p \text{ is outgoing}, \qquad x \in \partial\Omega_{\text{int}}, \tag{1.2}$$

$$p(x,0) = f(x), \qquad x \in \Omega_{\text{int}}, \tag{1.3}$$

$$\partial_t p(x,0) = g(x), \qquad x \in \Omega_{\text{int}}, \tag{1.4}$$

with initial conditions $f(x), g(x)$. The constant $c > 0$ is the wave speed. The radiation condition (1.2) should ensure that the solution p behaves like the solution of the problem on the whole space $\mathbb{R}^d$.

To define and realize the radiation condition we transform the wave equation (1.1) into the frequency domain via the Fourier transformation. This is done to be able to apply a frequency-dependent complex coordinate stretching to obtain exponentially decaying outgoing solutions.

Definition 1.1 (Fourier transformation). *Let $f \in L^1(\mathbb{R})$. Then the Fourier transformation of f is defined by* ([Jue15])

$$\hat{f}(k) := \mathcal{F}[f](k) = \int_{\mathbb{R}} f(x) e^{-ikx} \, \mathrm{d}x, \quad k \in \mathbb{R}.$$

The inverse Fourier transformation of $\hat{f}$ is given by

$$\mathcal{F}^{-1}[\hat{f}](x) = \frac{1}{2\pi} \int_{\mathbb{R}} \hat{f}(k) e^{ikx} \, \mathrm{d}k, \quad x \in \mathbb{R}.$$

With partial integration for a function $\phi \in C^\alpha(M)$ with $M \subset \mathbb{R}$, $\phi^{(\alpha)} \in L^1(M)$, and $\alpha \in \mathbb{N}$ it follows:

$$\widehat{\phi^{(\alpha)}}(k) = (-ik)^\alpha \hat{\phi}(k).$$

After the Fourier transformation is applied to the wave equation (1.1) in the time variable t, considering ω as a parameter, the transformed equation is the Helmholtz equation:

$$(-i\omega)^2\hat{p}(x,\omega) = c^2\Delta_x\hat{p}(x,\omega). \tag{1.5}$$

We observe that derivatives in the time variable t transform into multiplications with $-i\omega$.

Until now we have considered the problem on a bounded domain. After the transformation in the frequency space we expand the Helmholtz problem on the whole space, because we are interested in solutions, which do not reflect at a given boundary. Subsequently, we apply the Perfectly Matched Layer (PML) method, also called the complex scaling method or complex coordinate stretching, thus adding an absorbing layer surrounding the inner domain or interest, in which all initial values have compact support. This method is used to damp the solution and absorb the energy, which is transported outside of the inner domain, i.e. the complex scaling ensures exponential decay of the solution. After the is discretized in space, we apply the inverse Fourier transformation. Subsequently, an appropriate time stepping method is used. This corresponds to the vertical method of lines, i.e. the problem is first discretized in space and then in time.

When using well-known spatial discretization methods like finite difference or finite element methods, the computational domain needs to be truncated. The aim is thus to be able to truncate the PML layer domain at a point far enough from the boundary of the inner domain, such that no energy is reflected. A different variant for the spatial discretization of the outer domain is to use Hardy space infinite elements. For the time discretization we either use a second order time integration method or a linearization method to avoid usage of additional help functions.

The PML method was given its name by Bérenger (see [Ber94]) in the 90s, who used it for absorbing electromagnetic waves. Besides the complex scaling method, many techniques for artificial boundary conditions (ABCs) have been developed, among which are the high-order ABCs (see for example [Giv04,Nat13]). However, in this work only the PML method is introduced and used.

2 PML Method for the Helmholtz Equation

In this chapter the concept of complex scaling for the Helmholtz problem on the whole space is introduced. The variational formulation, which is later needed for the spatial discretization with finite elements, is derived and written in different coordinate systems.

We consider the transformed problem on an unbounded domain Ω,

$$(-i\omega)^2\hat{p}(x) - c^2\Delta\hat{p}(x) = 0, \qquad x \in \mathbb{R}^d, \tag{2.1}$$

$$\nabla_x(x) \cdot n = 0, \qquad x \in \partial\Omega, \tag{2.2}$$

$$\hat{p} \text{ fulfills a radiation condition for } |x| \to \infty. \tag{2.3}$$

We select an inner domain of interest Ω_{int}, which is a compact set with finite boundary and normal vector n directed outward. The radiation condition (2.3) is needed to ensure unique solvability of the Helmholtz equation. One possibility is the Sommerfeld radiation condition (see [Nan08],[Nan16]).

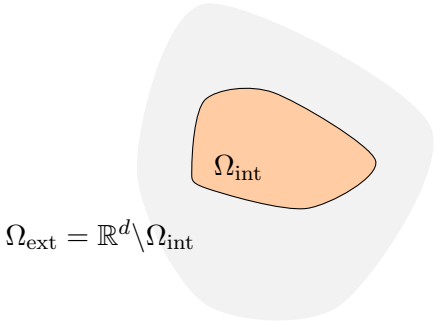

Figure 2.1: An example for domains for the Helmholtz problem (2.1) with $\Omega = \mathbb{R}^d$

The absorption of waves starts at the boundary of $\partial\Omega_{\text{int}}$ and is done with a complex scaling function, which is applied to the coordinate of the direction of the radiation. However, in the following sections we introduce different coordinate systems (cartesian, radial and curvilinear coordinates), and in each system the distinctive coordinate, which needs to be scaled, is different. The one-dimensional case is the simplest, because there is only one coordinate to scale. In higher dimensions different coordinate systems may be preferable depending on the shape of the computational domain, which is discussed further.

Figure 2.1 shows a possible configuration of the considered domains. The complex scaling starts at the boundary of Ω_{int}, in which all initial values have compact support. We thus define the rest of the whole space as the exterior domain $\Omega_{\text{ext}} := \mathbb{R}^d \backslash \Omega_{\text{int}}$. Next, we distinguish the coordinate of the direction of radiation, $\xi \in \mathbb{R}_+$ and consider a scaling function $\sigma(\omega) : \mathbb{C} \to \mathbb{C}$, which we apply in the following way

$$\xi \mapsto \sigma(\omega)\xi.$$

In Ω_{ext} the coordinate ξ is multiplied with the scaling function $\sigma(\omega)$, i.e. a function in $(-i\omega)$. How this leads to a damping of the solution of the Helmholtz problem is shown in Chapter 4. There are multiple ways to define the function $\sigma(\omega)$, thus changing the impact on the solutions of various wave-type equations. In this work we consider functions of the forms

$$\sigma_1(\omega) := \frac{\alpha}{-i\omega}, \tag{2.4}$$

$$\sigma_2(\omega) := \beta + \frac{\alpha}{-i\omega}, \tag{2.5}$$

$$\sigma_3(\omega) := \alpha_1 + \frac{\alpha_2 + \frac{\alpha_3}{-i\omega}}{\beta_1 - \beta_2 i\omega}, \tag{2.6}$$

with $\alpha, \beta, \alpha_i, \beta_i \in \mathbb{R}$. We call $\sigma_1(\omega)$ the vertical, $\sigma_2(\omega)$ the diagonal, and $\sigma_3(\omega)$ the convolutional scaling.

We define the complex scaled variable via a transformation

$$x \mapsto \gamma(x), \tag{2.7}$$

with γ depending on the choice of coordinate system and the scaling function $\sigma(\omega)$.

2.1 Weak formulation

The next step is to derive the complex scaled variational formulation for the Helmholtz equation in the three coordinate systems, as the weak formulation is further discretized with finite elements (see Chapter 3). First, consider the unscaled variational formulation of system (2.1-2.3) on the domain Ω. Multiplying (2.1) with test functions $\tilde{p} \in C_0^\infty(\Omega)$, and integrating over Ω yields

$$(-i\omega)^2 \int_\Omega \hat{p}(x)\tilde{p}(x)\ \mathrm{d}x - c^2 \int_\Omega \Delta\hat{p}(x)\tilde{p}(x)\ \mathrm{d}x = 0.$$

After partial integration, and including the boundary condition (2.2), we get

$$(-i\omega)^2 \int_\Omega \hat{p}(x)\tilde{p}(x)\ \mathrm{d}x + c^2 \int_\Omega \nabla\hat{p}(x) \cdot \nabla\tilde{p}(x)\ \mathrm{d}x = 0. \tag{2.8}$$

Note that in later sections other boundary conditions or a right hand side might be used.

The Jacobian of the scaling (2.7) is denoted by

$$J_\gamma(x) := \left(\frac{\partial \gamma((x_1, \dots, x_d)^T)}{\partial x_j} \right)_{i=1,\dots,d, j=1,\dots,d}.$$

We define the bilinear forms for $f, g \in H^1(\Omega)$, distinguishing between Ω_{int} and Ω_{ext}:

$$a_{\text{int}}(f,g) := \int_{\Omega_{\text{int}}} f(x)g(x)\ \mathrm{d}x, \tag{2.9}$$

$$a_{\text{ext}}(f,g) := \int_{\Omega_{\text{ext}}} f(x)g(x) \det J_\gamma(x)\ \mathrm{d}x, \tag{2.10}$$

$$b_{\text{int}}(f,g) := \int_{\Omega_{\text{int}}} \nabla f(x) \cdot \nabla g(x)\ \mathrm{d}x, \tag{2.11}$$

$$b_{\text{ext}}(f,g) := \int_{\Omega_{\text{ext}}} \Big(J_\gamma(x)^{-T} \nabla f(x) \Big) \cdot \Big(J_\gamma(x)^{-T} \nabla g(x) \Big) \det J_\gamma(x)\ \mathrm{d}x. \tag{2.12}$$

Within Ω_{int} the bilinear forms are not scaled. Hence, the variational formulation of (2.1-2.3) is stated as:

Problem 2.1. For fixed $\omega > 0$ find $\hat{p} \in H^1(\Omega)$, such that

$$c^2 b_{\text{int}}(\hat{p}, \tilde{p}) + c^2 b_{\text{ext}}(\hat{p}, \tilde{p}) = \omega^2 \big(a_{\text{int}}(\hat{p}, \tilde{p}) + a_{\text{ext}}(\hat{p}, \tilde{p}) \big), \tag{2.13}$$

for all test functions $\tilde{p} \in H^1(\Omega)$.

Depending on the choice of γ, the Jacobian J_γ and its determinant change accordingly. In the following sections we derive various choices for γ based on different coordinate systems.

2.2 Cartesian coordinates

In this section we consider the Helmholtz problem on $\mathbb{R}^2$ on a rectangular domain $\Omega_{\text{int}} = [-R_1, R_1] \times [-R_2, R_2]$ as shown in Figure 2.2. The concept can of course be applied to higher-dimensional problems. In this case the (x_1, x_2)-coordinates are scaled separately, since, depending on the position, the direction of radiation is either one or both of the two coordinates.

For $x = (x_1, x_2)$ we define the complex scaled variable as $\gamma(x) := (\gamma_1(x), \gamma_2(x))$ via

$$\gamma_j(x) := \begin{cases} {}_j\sigma(\omega) x_j, & x_j > R_j, \\ x_j, & x_j \in [-R_j, R_j], \\ -{}_j\sigma(\omega) x_j, & x_j < -R_j. \end{cases} \qquad j \in \{1, 2\},$$

We put the subscript of the scaling ${}_j\sigma$ on the left side merely to clarify that only the parameters α_i, β_i of the scaling may vary in each direction, and not that we use e.g. the vertical (σ_1) and the diagonal (σ_2) scaling in the same example.

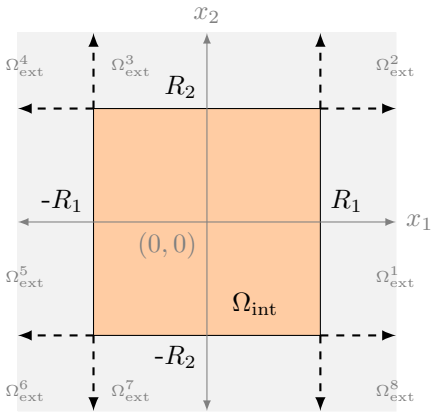

Figure 2.2: Cartesian coordinates

The Jacobian of the scaling is given by entries [PS10]:

$$J_\gamma(x) = \begin{pmatrix} \frac{\partial \gamma(x)}{\partial x_1} & 0 \\ 0 & \frac{\partial \gamma(x)}{\partial x_2} \end{pmatrix}, \tag{2.14}$$

with determinant $\det J_\gamma(x) = \frac{\partial \gamma(x)}{\partial x_1}\frac{\partial \gamma(x)}{\partial x_2}$. The exterior can be decomposed via $\Omega_{\text{ext}} = \cup_{i=1}^{8}\Omega^i_{\text{ext}}$.

For example, for $x = (x_1, x_2) \in \Omega^1_{\text{ext}}$ we have $\frac{\partial \gamma(x)}{\partial x_1} = {}_1\sigma(\omega)$ and $\frac{\partial \gamma(x)}{\partial x_2} = 1$. For $x \in \Omega^8_{\text{ext}}$ it holds $\frac{\partial \gamma(x)}{\partial x_1} = {}_1\sigma(\omega)$ and $\frac{\partial \gamma(x)}{\partial x_2} = -{}_2\sigma(\omega)$, i.e. the sign can be positive or negative. Furthermore, rewrite the bilinear forms for $f, g \in H^1(\Omega)$:

$$\begin{aligned}
a_{\text{ext}}(f,g) &= \int_{\Omega_{\text{ext}}} f(x)g(x)\frac{\partial \gamma(x)}{\partial x_1}\frac{\partial \gamma(x)}{\partial x_2}\,\mathrm{d}x, \\
b_{\text{ext}}(f,g) &= \int_{\Omega^1_{\text{ext}}} \left(\frac{1}{{}_1\sigma(\omega)}\frac{\partial f(x)}{\partial x_1}\frac{1}{{}_1\sigma(\omega)}\frac{\partial g(x)}{\partial x_1} + \frac{\partial f(x)}{\partial x_2}\frac{\partial g(x)}{\partial x_2}\right){}_1\sigma(\omega)\,\mathrm{d}x \\
&\quad + \int_{\Omega^2_{\text{ext}}} \left(\frac{1}{{}_1\sigma(\omega)}\frac{\partial f(x)}{\partial x_1}\frac{1}{{}_1\sigma(\omega)}\frac{\partial g(x)}{\partial x_1} + \frac{1}{{}_2\sigma(\omega)}\frac{\partial f(x)}{\partial x_2}\frac{1}{{}_2\sigma(\omega)}\frac{\partial g(x)}{\partial x_2}\right){}_1\sigma(\omega){}_2\sigma(\omega)\,\mathrm{d}x \\
&\quad + \sum_{i=3}^{8}\int_{\Omega^i_{\text{ext}}} \left(\left(\frac{\partial \gamma(x)}{\partial x_1}\right)^{-2}\frac{\partial f(x)}{\partial x_1}\frac{\partial g(x)}{\partial x_1} + \frac{\partial f(x)}{\partial x_2}\left(\frac{\partial \gamma(x)}{\partial x_2}\right)^{-2}\frac{\partial g(x)}{\partial x_2}\right)\frac{\partial \gamma(x)}{\partial x_1}\frac{\partial \gamma(x)}{\partial x_2}\,\mathrm{d}x.
\end{aligned}$$

One example of a cartesian PML is given in [KKS12], where only the three-dimensional case with the diagonal scaling function is discussed.

Compared to other coordinate systems the cartesian complex scaling is typically easy to implement. It is used to apply the PML method to problems where it is useful to define the interior domain as a rectangle.

2.3 Radial complex scaling

We further do not assume the domain of interest to be rectangular. For $d \in \{1, 2, 3\}$ let $\Omega \subset \mathbb{R}^d$ be an unbounded open domain and split it into an interior domain, a circle $\Omega_{\text{int}} = \Omega \cap B_R(0)$ with radius R and the center at the origin, and an unbounded exterior domain $\Omega_{\text{ext}} = \Omega \backslash \overline{\Omega_{\text{int}}}$ with interface $\Gamma = \partial B_R(0)$.

For each $x \in \Omega_{\text{ext}} \cup \Gamma$ there exists a unique pair $(\xi, \hat{\mathbf{x}}) \in \mathbb{R}_+ \times \Gamma$, such that

$$x = x(\xi, \hat{\mathbf{x}}) = \left(1 + \frac{\xi}{R}\right) \hat{\mathbf{x}}.$$

We write $\xi(x)$ and $\hat{\mathbf{x}}(x)$ for the inverse mappings.

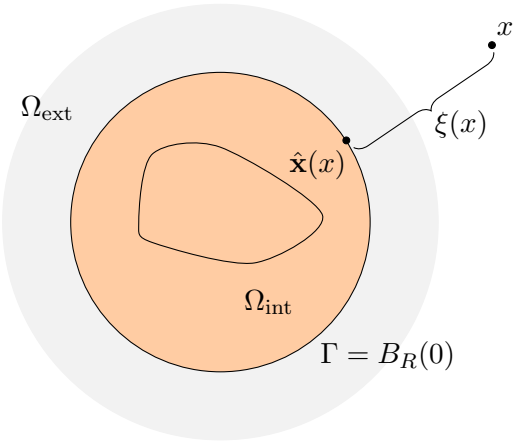

Figure 2.3: Radial PML

Figure 2.3 illustrates this setting. In correspondance to considerations from before, we have that ξ is the variable of the direction of radiation. We further define the complex scaled variable

$$\gamma(x) := \begin{cases} x, & x \in \Omega_{\text{int}}, \\ x(\sigma(\omega)\xi, \hat{\mathbf{x}}), & x \in \Omega_{\text{ext}}. \end{cases}$$

Now, we can formulate the variational formulation of problem (2.1) on the whole space.

2.3.1 2D example in polar coordinates

The use of a radial scaling in the two-dimensional case suggests to transform the problem into polar coordinates and only apply the scaling to the radial component. We parametrize the interface Γ by:

$$\hat{\mathbf{x}} = \varphi(\eta) = R \begin{pmatrix} \cos \eta \\ \sin \eta \end{pmatrix},$$

for $\eta \in (-\pi, \pi)$. Next, we consider the coordinate transformation $\Psi_\varphi : \mathbb{R}_+ \times (-\pi, \pi) \to \Omega_{\text{ext}} \cup \Gamma$:

$$\Psi_\varphi(\xi, \eta) = \left(1 + \frac{\xi}{R}\right) \varphi(\eta).$$

We have that

$$D\varphi(\eta) = R \begin{pmatrix} -\sin\eta \\ \cos\eta \end{pmatrix}.$$

The Jacobian and its inverse are given by

$$D\Psi_\varphi(\xi, \eta) = \left(\frac{1}{R}\varphi(\eta), \left(1 + \frac{\xi}{R}\right) D\varphi(\eta)\right) = \begin{pmatrix} R\cos\eta & -(R+\xi)\sin\eta \\ R\sin\eta & (R+\xi)\cos\eta \end{pmatrix},$$
$$(D\Psi_\varphi(\xi, \eta))^{-1} = \begin{pmatrix} \frac{1}{R}\cos\eta & \frac{1}{R}\sin\eta \\ -\frac{1}{R+\xi}\sin\eta & \frac{1}{R+\xi}\cos\eta \end{pmatrix}$$

The determinant is calculated as (see [NW19]):

$$|\det D\Psi_\varphi(\xi, \eta)| = \left(1 + \frac{\xi}{R}\right) \sqrt{|\det (D\varphi(\eta)^T D\varphi(\eta))|} = \left(1 + \frac{\xi}{R}\right) R.$$

Further, we define the surface gradient of a function $f : \Gamma \to \mathbb{C}$:

$$\nabla_\Gamma f(\varphi(\eta)) := \frac{1}{R^2 + R\xi} \begin{pmatrix} -\sin\eta \\ \cos\eta \end{pmatrix} \nabla_\eta (f \circ \varphi)(\eta). \tag{2.15}$$

We have that

$$\gamma(\Psi_\varphi(\xi, \eta)) = \Psi_\varphi(\sigma(\omega)\xi, \eta),$$

and combining the coordinate transformation and the scaling results in:

$$D(\gamma \circ \Psi_\varphi)(\xi, \eta) = D\Psi_\varphi(\sigma(\omega)\xi, \eta) \begin{pmatrix} \sigma(\omega) & 0 \\ 0 & 1 \end{pmatrix},$$
$$(D(\gamma \circ \Psi_\varphi)(\xi, \eta))^{-1} = \begin{pmatrix} \frac{1}{\sigma(\omega)} & 0 \\ 0 & 1 \end{pmatrix} (D\Psi_\varphi(\sigma(\omega)\xi, \eta))^{-1},$$
$$\det D(\gamma \circ \Psi_\varphi)(\xi, \eta) = \sigma(\omega) \det D\Psi_\varphi(\sigma(\omega)\xi, \eta).$$

Let $f, g \in H^1(\Omega)$. The exterior bilinear forms of the variational formulation (2.13) can now be written in the coordinates $\xi, \hat{\mathbf{x}}$:

$$a_{\text{ext}}(f, g) = \sigma(\omega) \int_{\mathbb{R}_+ \times \Gamma} f(x(\xi, \hat{\mathbf{x}})) g(x(\xi, \hat{\mathbf{x}})) \left(1 + \frac{\sigma(\omega)\xi}{R}\right) \, \mathrm{d}(\xi, \hat{\mathbf{x}}),$$
$$b_{\text{ext}}(f, g) = \frac{1}{\sigma(\omega)} \int_{\mathbb{R}_+ \times \Gamma} \frac{\partial f}{\partial \xi}(x(\xi, \hat{\mathbf{x}})) \frac{\partial g}{\partial \xi}(x(\xi, \hat{\mathbf{x}})) \left(1 + \frac{\sigma(\omega)\xi}{R}\right) \, \mathrm{d}(\xi, \hat{\mathbf{x}})$$
$$+ \sigma(\omega) \int_{\mathbb{R}_+ \times \Gamma} \nabla_\Gamma f(x(\xi, \hat{\mathbf{x}})) \cdot \nabla_\Gamma g(x(\xi, \hat{\mathbf{x}})) \frac{1}{1 + \frac{\sigma(\omega)\xi}{R}} \, \mathrm{d}(\xi, \hat{\mathbf{x}}).$$

The integration over Γ of a function $h : \Gamma \to \mathbb{C}$ can be understood as:

$$\int_\Gamma h(\hat{\mathbf{x}})\ \mathrm{d}\hat{\mathbf{x}} = \int_{\varphi((-\pi,\pi))} h(\varphi(\eta))R\ \mathrm{d}\eta.$$

To separate the equation in radial and tangential components, we introduce a help function

$$u(x(\xi,\hat{\mathbf{x}})) = \frac{\nabla_\Gamma g(x(\xi,\hat{\mathbf{x}}))}{1+\frac{\sigma(\omega)\xi}{R}}.$$

In weak form we obtain the system in Ω_{ext}:

$$\begin{aligned}
&\frac{1}{\sigma(\omega)}\int_{\mathbb{R}_+\times\Gamma}\frac{\partial f}{\partial\xi}(x(\xi,\hat{\mathbf{x}}))\frac{\partial g}{\partial\xi}(x(\xi,\hat{\mathbf{x}}))\left(1+\frac{\sigma(\omega)\xi}{R}\right)\ \mathrm{d}(\xi,\hat{\mathbf{x}})\\
&\qquad+\sigma(\omega)\int_{\mathbb{R}_+\times\Gamma}\nabla_\Gamma f(x(\xi,\hat{\mathbf{x}}))u(x(\xi,\hat{\mathbf{x}}))\ \mathrm{d}(\xi,\hat{\mathbf{x}})\\
&-\omega^2\sigma(\omega)\int_{\mathbb{R}_+\times\Gamma} f(x(\xi,\hat{\mathbf{x}}))g(x(\xi,\hat{\mathbf{x}}))\left(1+\frac{\sigma(\omega)\xi}{R}\right)\ \mathrm{d}(\xi,\hat{\mathbf{x}})=0.
\end{aligned}$$

$$\int_{\mathbb{R}_+\times\Gamma}\left(1+\frac{\sigma(\omega)\xi}{R}\right)u(x(\xi,\hat{\mathbf{x}}))\tilde{u}(x(\xi,\hat{\mathbf{x}}))\ \mathrm{d}(\xi,\hat{\mathbf{x}})-\int_{\mathbb{R}_+\times\Gamma}\nabla_\Gamma g(x(\xi,\hat{\mathbf{x}}))\tilde{u}(x(\xi,\hat{\mathbf{x}}))\ \mathrm{d}(\xi,\hat{\mathbf{x}})=0,$$

2.4 Curvilinear coordinates

We want to be able to allow inhomogeneities of the boundary of the domain of interest, but not necessarily restrict ourselves to rectangular domains, which would need the cartesian complex scaling, or to circular domains for which we could use radial coordinates.

Curvilinear coordinates generate a special coordinate system often used in differential geometry, and are a generalization of orthogonal polar coordinates. In order to write the variational formulation of the Helmholtz problem in this coordinate system we have to rewrite the gradient in curvilinear coordinates, and then apply the complex scaling. In the following we introduce the overall concept of curvilinear coordinates for arbitrary dimension $d \in \mathbb{N}$ and further implement it in the two-dimensional case.

Let Ω_{int} be a convex bounded domain in $\mathbb{R}^d$, $\Gamma = \partial\Omega_{\text{int}}$ a smooth manifold in $\mathbb{R}^{d-1}$ with outer normal n, such that the mapping

$$\Psi : \begin{cases} \mathbb{R}_+ \times \Gamma & \to \Omega_{\text{ext}} = \mathbb{R}^d \backslash \Omega_{\text{int}}, \\ (\xi, \hat{\mathbf{x}}) & \mapsto \hat{\mathbf{x}} + \xi n(\hat{\mathbf{x}}), \end{cases} \tag{2.16}$$

is a bijection. Let the diffeomorphism φ be a parametrization

$$\varphi : \begin{cases} M & \to \Gamma, \\ \eta & \mapsto \hat{\mathbf{x}}, \end{cases} \tag{2.17}$$

such that the columns of $D\varphi(\eta) = (\tau_i)_{i=1,\dots,d-1}$ are orthonormal tangential vectors τ_i. This embedding goes from a set $M \in \mathbb{R}^{d-1}$ to the manifold Γ, and corresponds to the embedding

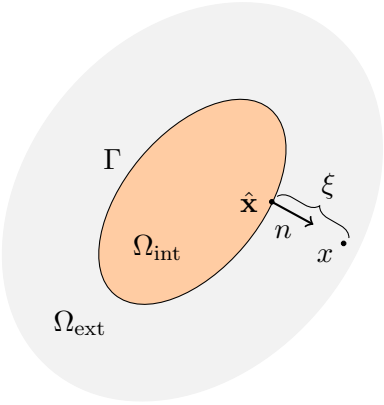

Figure 2.4: Curvilinear coordinates

in the foregoing section.

We can write

$$D(n \circ \varphi(\eta)) = D\varphi(\eta)(\kappa_i(\varphi(\eta))) = (\tau_1\kappa_1(\varphi(\eta)), \ldots, \tau_{d-1}\kappa_{d-1}(\varphi(\eta))), \tag{2.18}$$

with curvatures κ_i. Furthermore, define the function $\Psi_\varphi : \mathbb{R}_\times M+ \to \mathbb{R}^d$,

$$\Psi_\varphi(\xi, \eta) := \Psi(\xi, \varphi(\eta)), \tag{2.19}$$

and compute its Jacobian, inverse Jacobian and determinant, which we make use of later on,

$$\begin{aligned}
J(\xi,\eta) &:= D\Psi_\varphi(\xi, \varphi(\eta)) = (n(\varphi(\eta)), (1 + \kappa(\varphi(\eta)))D\varphi(\eta)) \\
J^{-1}(\xi,\eta) &= \operatorname{diag}\left(n(\varphi(\eta)), \tau_1(\varphi(\eta))\frac{1}{1+\kappa_1(\varphi(\eta))\xi}, \ldots, \tau_{d-1}(\hat{\mathbf{x}})\frac{1}{1+\kappa_{d-1}(\varphi(\eta))\xi}\right)^T, \\
\det J(\xi,\eta) &= \prod_{i=1}^{d-1}(1+\kappa_i(\varphi(\eta))\xi)\sqrt{|\det\left(D\varphi(\eta)^T D\varphi(\eta)\right)|}.
\end{aligned}$$

The gradient of a function h in curvilinear coordinates can be written as

$$\begin{aligned}
\nabla_x h = J^{-T}\nabla_{(\xi,\eta)}h &= n\frac{\partial}{\partial\xi}h + D\varphi(\eta)\ \operatorname{diag}\left(\frac{1}{1+\kappa_1\xi}, \ldots, \frac{1}{1+\kappa_{d-1}\xi}\right) D\varphi(\eta)^T\nabla_\Gamma h \\
&= n\frac{\partial}{\partial\xi}h + \sum_{i=1}^{d-1}\frac{1}{1+\kappa_i\xi}\tau_i\tau_i^T\nabla_\Gamma h,
\end{aligned}$$

where we used the surface gradient ∇_Γ defined for a function $f : \Gamma \to \mathbb{C}$ via:

$$\nabla_\Gamma f(\varphi(\eta)) := \left(D\varphi(\eta)^\dagger\right)^T \nabla_\eta(f \circ \varphi)(\eta), \tag{2.20}$$

whereas $A^\dagger := (A^T A)^{-1} A^T$ denotes the pseudo inverse of a matrix $A \in \mathbb{C}^{d \times d-1}$ with full rank. The transformed integrals of the Helmholtz problem on a bounded domain for $a, b \in \mathbb{R}$ can now be written as

$$\begin{aligned}\int_{\Psi((a,b)\times\Gamma)} \nabla\hat{p}(x) \cdot \nabla\tilde{p}(x)\ \mathrm{d}x &= \int_{(a,b)\times\Gamma} \frac{\partial\hat{p}}{\partial\xi}(\xi,\hat{\mathbf{x}}) \frac{\partial\tilde{p}}{\partial\xi}(\xi,\hat{\mathbf{x}}) \prod_{i=1}^{d-1}(1+\kappa_i(\hat{\mathbf{x}})\xi)\ \mathrm{d}(\xi,\hat{\mathbf{x}}) \\ &\quad + \int_{(a,b)\times\Gamma} \sum_{i=1}^{d} \prod_{i\neq j} \frac{1+\kappa_j(\hat{\mathbf{x}})\xi}{1+\kappa_i(\hat{\mathbf{x}})\xi} \nabla_\Gamma\hat{p}(\xi,\hat{\mathbf{x}}) \cdot \tau_i \nabla_\Gamma\tilde{p}(\xi,\hat{\mathbf{x}}) \cdot \tau_i\ \mathrm{d}(\xi,\hat{\mathbf{x}}), \\ \omega^2 \int_{\Psi((a,b)\times\Gamma)} \hat{p}(x)\tilde{p}(x)\ \mathrm{d}x &= \omega^2 \int_{(a,b)\times\Gamma} \prod_{i=1}^{d-1}(1+\kappa_i(\hat{\mathbf{x}})\xi)\hat{p}(\xi,\hat{\mathbf{x}})\tilde{p}(\xi,\hat{\mathbf{x}})\ \mathrm{d}(\xi,\hat{\mathbf{x}}),\end{aligned}$$

whereas the integration over Γ of a function $h : \Gamma \to \mathbb{C}$ can be understood as

$$\int_\Gamma h(\hat{\mathbf{x}})\ \mathrm{d}\hat{\mathbf{x}} = \int_{\varphi(M)} h(\phi(\eta)) \sqrt{|\det\left(D\varphi(\eta)^T D\varphi(\eta)\right)|}\ \mathrm{d}\eta.$$

Example in 2D: In the two-dimensional case we have only one curvature κ and one tangential vector τ, an it thus holds

$$\begin{aligned} D\Psi_\varphi(\xi,\eta) &= (n(\varphi(\eta)), \tau(1+\kappa(\varphi(\eta))\xi)), \\ \det D\Psi_\varphi(\xi,\eta) &= 1+\kappa(\hat{\mathbf{x}})\xi, \end{aligned}$$

such that we can write the Helmholtz problem as

$$\begin{aligned}\int_{(a,b)\times\Gamma} \left(\frac{\partial\hat{p}}{\partial\xi}(\xi,\hat{\mathbf{x}}) \frac{\partial\tilde{p}}{\partial\xi}(\xi,\hat{\mathbf{x}})(1+\kappa(\hat{\mathbf{x}})\xi) + \frac{1}{1+\kappa(\hat{\mathbf{x}})\xi} \nabla_\Gamma\hat{p}(\xi,\hat{\mathbf{x}}) \cdot \tau \nabla_\Gamma\tilde{p}(\xi,\hat{\mathbf{x}}) \cdot \tau \right)\ \mathrm{d}(\xi,\hat{\mathbf{x}}) = \\ \omega^2 \int_{(a,b)\times\Gamma} (1+\kappa(\hat{\mathbf{x}})\xi)\hat{p}(\xi,\hat{\mathbf{x}})\tilde{p}(\xi,\hat{\mathbf{x}})\ \mathrm{d}(\xi,\hat{\mathbf{x}}).\end{aligned} \tag{2.21}$$

The next step is to apply a complex scaling to the to the radial coordinate, $\xi \mapsto \sigma(\omega)\xi$, in the transformed equation (2.21). The scaling functions $\sigma(\omega)$ have the same structures as mentioned in the foregoing Section 2. The thus defined function $\gamma_{\sigma,\varphi}(\xi,\eta) := \Psi(\sigma(\omega)\xi,\hat{\mathbf{x}})$ has the Jacobian $J_\gamma = D\gamma_{\sigma,\varphi} = \Big(n, \tau(1+\kappa\sigma(\omega)\xi)\Big)$. For the next step we omit the arguments to simplify the notation. Applying the complex scaling to the transformed equation (2.21) yields

$$\begin{aligned}\int_{\mathbb{R}_+\times\Gamma} \left(\frac{\partial\hat{p}}{\partial\xi} \frac{\partial\tilde{p}}{\partial\xi} \frac{1+\kappa\sigma(\omega)\xi}{\sigma(\omega)} + \frac{\sigma(\omega)}{1+\kappa\sigma(\omega)\xi} \nabla_\Gamma\hat{p} \cdot \tau \nabla_\Gamma\tilde{p} \cdot \tau \right)\ \mathrm{d}(\xi,\hat{\mathbf{x}}) = \\ \omega^2 \int_{\mathbb{R}_+\times\Gamma} \sigma(\omega)(1+\kappa\sigma(\omega)\xi)\hat{p}\tilde{p}\ \mathrm{d}(\xi,\hat{\mathbf{x}}).\end{aligned} \tag{2.22}$$

In order to separate the system in integrals of tangential and normal parts we introduce an additional variable u via

$$i\omega u\sigma(\omega) = \frac{\nabla_\Gamma \hat{p}\cdot\tau}{1+\kappa\sigma(\omega)\xi}\sigma(\omega).$$

This leads to a system with test function $\tilde{u}$ corresponding to u,

$$\begin{aligned}\int_{\mathbb{R}_+\times\Gamma} \frac{\partial\hat{p}}{\partial\xi}\frac{\partial\tilde{p}}{\partial\xi}\frac{1+\kappa\sigma(\omega)\xi}{\sigma(\omega)}\,\mathrm{d}(\xi,\hat{\mathbf{x}}) + i\omega\int_{\mathbb{R}_+\times\Gamma}\sigma(\omega)u\cdot\nabla_\Gamma\tilde{p}\cdot\tau\,\mathrm{d}(\xi,\hat{\mathbf{x}})\\ +(-i\omega)^2\int_{\mathbb{R}_+\times\Gamma}\sigma(\omega)(1+\kappa\sigma(\omega)\xi)\hat{p}\tilde{p}\,\mathrm{d}(\xi,\hat{\mathbf{x}}) = 0, \quad (2.23)\\ (-i\omega)^2\int_{\mathbb{R}_+\times\Gamma}(1+\kappa\sigma(\omega)\xi)u\cdot\tilde{u}\sigma(\omega)\,\mathrm{d}(\xi,\hat{\mathbf{x}}) + i\omega\int_{\mathbb{R}_+\times\Gamma}\nabla_\Gamma\hat{p}\cdot\tau\cdot\tilde{u}\sigma(\omega)\,\mathrm{d}(\xi,\hat{\mathbf{x}}) = 0.\end{aligned}$$

In the subsequent chapters the behavior of different scalings $\sigma(\omega)$ is considered based on this system in curvilinear coordinates.

3 Discretization

To discretize the Problem (2.1) for cartesian, radial and curvilinear coordintaes in space and time, we use finite elements in space in Ω_{int} and different time discretization methods. The exterior domain is either discretized with finite elements or Hardy space based infinite elements.

3.1 Finite Elements in Ω_{int}

The spatial discretization in the inner domain is done using the Finite Element Method (FEM) (see e.g. [Cia78]). It aims to find a solution of the variational problem (2.13) on a finite-dimensional subspace X_h of the solution space X:

$$\hat{p}_h \in X_h \text{ solves} \quad b_{\text{int}}(\hat{p}_h, \tilde{p}_h) = \omega^2 a_{\text{int}}(\hat{p}_h, \tilde{p}_h), \qquad \tilde{p}_h \in X_h. \tag{3.1}$$

We decompose the domain Ω_{int} into elements T of the triangulation $\mathcal{T} = \{T\}$ and the set of nodes $\mathcal{N} = \{x_j\}$. Common elements are trianlges and quadrilaterals (2D) or tetrahedra, hexahedra and pentahedra (3D) forming a mesh. They can be designed following the prerequisites from [Cia78]. By means of this setting we define the finite element space X_h (see [Sch18]) of order $k \in \mathbb{N}$:

$$X_h := \{v \in C(\Omega_{\text{int}}) : v|_T \text{ is a polynomial of order } k \ \forall T \in \mathcal{T}\}$$

Moreover, we choose a basis $\{\psi_i\}_{i=1,\dots,N}$ of X_h, and we can write the solution of problem (3.1) as $\hat{p}_h = \sum_{i=1}^{N} u_i \psi_i \in X_h$. The basis functions are defined with a support $\text{supp}(\psi_i) = \overline{\{x \in \Omega \mid \psi_i(x) \neq 0\}}$, which is as small as possible. A convenient choice of basis functions is the nodal basis via $\psi_i(x_j) = \delta_{i,j}$ with the Kronecker-δ. We further define the matrices

$$A_h = (a_{i,j})_{i,j=1,\dots,N} \text{ with } a_{i,j} := a_{\text{int}}(\psi_i, \psi_j),$$
$$B_h = (b_{i,j})_{i,j=1,\dots,N} \text{ with } b_{i,j} := b_{\text{int}}(\psi_i, \psi_j),$$

and $u_h := (u_i, \dots, u_N)^T$ solves the system of equations:

$$(A_h - \omega^2 B_h) u_h = 0.$$

Different basis functions have disjoint support on the triangulation, and non-corresponding entries in A_h and B_h vanish, such that the matrices are sparse.

3.2 Infinite Elements in Ω_{ext}

An option would be to also use finite elements for the exterior domain, which is done for the implementation of the examples in 1D. However, this method produces an additional truncation error.

To avoid the truncation error, we use infinite elements based on Hardy space infinite elements (see [NW19],[HL09]). The exterior coordinates $\xi, \hat{\mathbf{x}}$ and a tensor product ansatz space is used. Figure (3.1) illustrates this idea. The space is composed of boundary functions as traces of interior basis functions, and basis functions in the normal coordinate:

$$\phi_j(\xi) = \exp(-\xi)p_j(\xi), \qquad j = 0, \dots, N,$$

with special polynomials p_j of degree j for some $N \in \mathbb{N}$. The interior and exterior discrete space need to be coupled, such that the resulting space is equivalent to a subspace of $H^1(\Omega)$. To obtain this we indentify an interior basis function with non-vanishing trace on Γ with an exterior basis function.

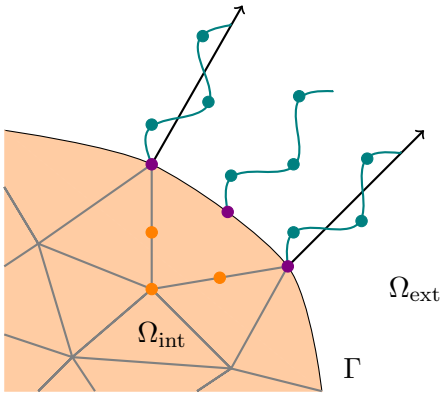

Figure 3.1: Tensor product basis, and degrees of freedom for triangular finite elements of order 2 and infinite elements of order 3.

By means of discretization we get a system of equations of the form

$$\sum_i q_i(-i\omega)M_i u_h(t) = 0, \tag{3.2}$$

for $i = 1, \dots, k, k \in \mathbb{N}$ with rational functions q_i.

3.3 Transformation in time domain

The inverse Fourier transformation (1.1) takes the complex scaled system (3.2) from the frequency space back to the time domain, where multiplications with $(-i\omega)$ transform into derivatives in time. The resulting equation can be written as

$$\sum_i q(\partial_t)M_i u_h(t) = 0, \tag{3.3}$$

i.e. as a sum of rational functions q_i in derivatives of time multiplied with correspondent matrices and solution vectors for $i = 1, \dots, k, k \in \mathbb{N}$. Due to the fact that q_i are rational, we have various options concerning the time discretization. We can write this equation as a first or second order system and define additional functions to dispose of fractions with time derivations in the denominator. Both concepts are introduced below.

3.4 Linearization

The wave problem includes second order time derivatives. Applying the complex scalings to the transformed Helmholtz problem and transforming back from the frequency space can, as seen above, leave the variational formulation with terms with time derivatives in the denominator. It can thus become rather difficult to skillfully design help functions in order to avoid those terms. To handle this problem, we thus introduce a method to linearize the second order problem and then use the implicit Euler method.

As an example consider the following problem for $M_0, M_1, M_2 \in \mathbb{C}^{n\times n}, u, f \in \mathbb{C}^n$:

$$M_0 u(t) + M_1 \partial_t u(t) + M_2 \partial_t^2 u(t) = f(t).$$

For ease of notation, write

$$M_0 u + M_1 u' + M_2 u'' = f. \tag{3.4}$$

Introducing $v := u'$ leads to the new system,

$$\begin{aligned} M_0 u + M_1 v + M_2 v' &= f, \\ u' - v &= 0. \end{aligned}$$

This can be equivalently written as

$$\begin{pmatrix} M_0 & M_1 \\ 0 & -I_n \end{pmatrix} \begin{pmatrix} u \\ v \end{pmatrix} + \begin{pmatrix} 0 & M_2 \\ I_n & 0 \end{pmatrix} \begin{pmatrix} u' \\ v' \end{pmatrix} = 0.$$

We thus define the matrices

$$\hat{\mathbf{M}} := \begin{pmatrix} M_0 & M_1 \\ 0 & -I_n \end{pmatrix}, \quad \tilde{\mathbf{M}} := \begin{pmatrix} 0 & M_2 \\ I_n & 0 \end{pmatrix},$$

with which we can rewrite the problem as a first order equation,

$$(\hat{\mathbf{M}} + \partial_t \tilde{\mathbf{M}})\mathbf{u}(t) = \mathbf{f}(t),$$

with $\hat{\mathbf{M}}, \tilde{\mathbf{M}} \in \mathbb{C}^{2n\times 2n}, \mathbf{f}(t), \mathbf{u}(t) \in \mathbb{C}^{2n}$. Furthermore, we can use first order time integration methods such as the implicit Euler method.

The implicit Euler method for some start vector $\mathbf{u}_0 \in \mathbb{C}^n$ and time step $\tau \in \mathbb{R}_+$ is defined by

$$\mathbf{u}_{i+1} := \mathbf{u}_i - \tau(\tilde{\mathbf{M}} + \tau\hat{\mathbf{M}})^{-1}(\hat{\mathbf{M}}u_i - \mathbf{f}_{i+1}) = \mathbf{E}(\mathbf{u}_i, \mathbf{f}_{i+1}, \tau), \tag{3.5}$$

where $\mathbf{f}_i := \mathbf{f}(i\tau)$. For our purposes, the right hand side f may be equal to zero. In each step of the Euler method we have to apply the inverse of $(\tilde{\mathbf{M}} + \tau\hat{\mathbf{M}})$ to a given vector.

The motivation for using this method rather than some second order time integration is that it enables us to solve systems like

$$M_0 u + M_1 u' + M_2 u'' + A\frac{1}{\alpha + \beta\partial_t} u = 0, \tag{3.6}$$

or systems with more complex terms of powers of time derivatives in the denominator without having to introduce new help functions in the variational framework. As an example set $\alpha, \beta = 1$ and $A = I_n$. Introducing

$$\begin{aligned} v &= u', \\ u - \alpha a &= \beta a', \end{aligned}$$

yields

$$\hat{\mathbf{M}} = \begin{pmatrix} M_0 & M_1 & A \\ 0 & I_n & 0 \\ I_n & 0 & -\alpha I_n \end{pmatrix}, \quad \tilde{\mathbf{M}} = \begin{pmatrix} 0 & M_2 & 0 \\ -I_n & 0 & 0 \\ 0 & 0 & -\beta I_n \end{pmatrix}.$$

Due to the special structure of the matrix $(\tilde{\mathbf{M}} + \tau\hat{\mathbf{M}})$ the application of its inverse can be realized using a Schur complement. This reduces the inversion of the large matrix of dimension $3n \times 3n$ to the inversion of a $n \times n$ matrix. Note that this is independent of the number of additional variables needed to linearize the given problem.

To this end we implement a Python class with the following functions:

```
class IELP(TimeIntegrator):
   '''Implicit Euler for linearizable Problems'''

   def __init__(self,Vh,Vt,Sh,St,tau,u0,f=None):
     ...

   def InvertSchurComp(self,inversetype,freedofs = None):
     # realize the inversion of the Schur complement
     ...

   def Step(self):
     # one time step of the implicit Euler
     ...
```

According to the motivational example above we assign the values, partitioning $\hat{\mathbf{M}}$ and $\tilde{\mathbf{M}}$:

$$\texttt{Vh} = [M_0, M_1, A], \qquad \texttt{Vt} = [\texttt{None}, M_2, \texttt{None}],$$
$$\texttt{Sh} = \texttt{array}([[0,1,0],[1,0,-\alpha]), \qquad \texttt{St} = \texttt{array}([[-1,0,0],[0,0,\beta]]).$$

We then call the function `IELP(Vh,Vt,Sh,St,tau,u0)` and optional source term with time step `tau` and initial value `u0`:

```
timeint = IELP(Vh,Vt,Sh,St,tau,u0)

timeint.InvertSchurComp()
i = 0
while True:
   timeint.Step()
   Redraw()
   i += 1
```

The inversion of the Schur complement is done only once.

3.5 Second order time integration

Instead of linearizing and using the implicit Euler method we can write (3.6) as a second order problem and use a time-integrator for second order problems. For the one-dimensional problems we further use the following second order method and employ the linearization method to the two-dimensional cases.

We now introduce a second order time integration method of the following structure. Consider the problem

$$M_0 u + M_1 u' + M_2 u'' = 0. \tag{3.7}$$

We use the approximations

$$\begin{aligned} u(t_i) &\approx u_i = \frac{u_{i+1} + 2u_i + u_{i-1}}{4}, \\ u'(t_i) &\approx u_i' = \frac{u_{i+1} - u_{i-1}}{2\tau}, \\ u''(t_i) &\approx u_i'' = \frac{u_{i+1} - 2u_i + u_{i-1}}{\tau^2}, \end{aligned}$$

and define the matrices

$$\begin{aligned} A &:= \frac{\tau^2}{4} M_0 + \frac{\tau}{2} M_1 + M_2, \\ B &:= \frac{\tau^2}{2} M_0 - 2M_2, \\ C &:= \frac{\tau^2}{4} M_0 - \frac{\tau}{2} M_1 + M_2, \end{aligned}$$

such that it holds

$$A u_{i+1} + b u_i + C u_{i-1} = 0.$$

After reformulation we get

$$u_{i+1} = -A^{-1} B u_i - A^{-1} C u_{i-1}.$$

For small time steps τ it is thus crucial to ensure invertibility of the matrix A, which is approximately M_2 for small time steps. In Chapter 4 we see how one can choose (possibly needed) help functions to provide invertibility. We will see in Chapter 6 that the linearization method proves to be much faster regarding computational costs.

4 1D Klein-Gordon and Wave Equation

The aim of this chapter is to write the variational formulation for the complex scaled Klein-Gordon problem in one dimension with the scaling functions $\sigma_i(\omega)$ (2.4) from before.

4.1 Motivation

The motivation for considering the so-called Klein-Gordon equation comes from wave guides in more dimensions, where the equation is implicitly included. To derive the Klein-Gordon equation we examine the Helmholtz equation in two dimensions on a wave guide with the shape:

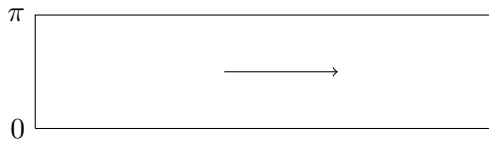

By separation of variables the unknown of the Helmholtz problem can be split into the two cartesian coordinates, $\hat{p}(x,y) = p(x)q(y)$, and we can write the Helmholtz equation (with wave speed $c \equiv 1$) as:

$$-\Delta_{(x,y)}p(x)q(y) - \omega^2 p(x)q(y) = 0.$$

Additional calculation yields

$$-p''(x)q(y) - p(x)q''(y) - \omega^2 p(x)q(y) = 0. \tag{4.1}$$

Dividing by $p(x)q(y)$ gives

$$-\frac{p''(x)}{p(x)} - \omega^2 = -\frac{q''(y)}{q(y)} \equiv \text{const.}$$

This leads to the eigenvalue problem for $y \in [0,\pi]$,

$$-q''(y) = \lambda q(y),$$

solved by $q(y) = \cos(ny), n^2 = \lambda, n \in \mathbb{N}$. Integrating this into the equation (4.1) yields

$$-p''(x)\cos(ny) + p(x)n^2\cos(ny) - \omega^2 p(x)\cos(ny) = 0,$$

which can be written as

$$-p''(x) - (\omega^2 - n^2)p(x) = 0. \tag{4.2}$$

Equation (4.2) is the so-called Klein-Gordon equation, which reads as the Helmholtz equation for wave numbers $k_n(\omega) = \sqrt{\omega^2 - n^2}$ (and not only $k_n(\omega) = \sqrt{\omega^2}$).

4.2 The problem

Let $\Omega = \Omega_{\text{int}} \cup \Omega_{\text{pml}} \subset \mathbb{R}$ a bounded domain and the interface $\Gamma = \overline{\Omega_{\text{int}}} \cap \overline{\Omega_{\text{pml}}}$. In this chapter we consider the following version of the so-called Klein-Gordon equation in space and time in one dimension:

$$\frac{1}{c^2}\partial_t^2 p(x,t) = \partial_x^2 p(x,t) - \text{pot}(x)^2 p(x,t), \qquad x \in \Omega, t \in [0,T], \tag{4.3}$$

$$\partial_x p(x,t) = 0, \qquad x \in \partial\Omega, t \in [0,T], \tag{4.4}$$

$$p(x,0) = f(x), \qquad x \in \Omega_{\text{int}}, \tag{4.5}$$

$$\partial_t p(x,0) = g(x), \qquad x \in \Omega_{\text{int}}, \tag{4.6}$$

which reads as the wave equation with the additional potential term $-\text{pot}(x)^2 p(x,t)$, $\mathbb{R} \supset T > 0$, and wave speed $c > 0$. The initial conditions f, g have compact support in Ω_{int}. The Klein-Gordon equation corresponds to (4.2) in the motivation above.

After the Fourier transformation is applied to the equation (4.3) in the time variable t, considering $\omega \in \mathbb{R}$ as a parameter, the transformed equation (with wave speed $c \equiv 1$) reads

$$(i\omega)^2 \hat{p}(x,\omega) = \partial_x^2 \hat{p}(x,\omega) - \text{pot}(x)^2 \hat{p}(x,\omega),$$

which can be rewritten as

$$-\partial_x^2 \hat{p}(x) - (\omega^2 - \text{pot}(x)^2)\hat{p}(x) = 0. \tag{4.7}$$

Solutions of the Helmholtz equation have the form

$$\hat{p}(x) = \exp(i\sqrt{\omega^2}x),$$

and, if we define the potential term as a constant function, the solutions of the Klein-Gordon equation have the representations

- $\omega > \text{pot} \Longrightarrow \hat{p}(x) = \exp(i\sqrt{\omega^2 - \text{pot}^2}x)$
- $\omega < \text{pot} \Longrightarrow \hat{p}(x) = \exp(-\sqrt{\text{pot}^2 - \omega^2}x)$

The next step is to derive the variational formulations of the Klein-Gordon and the Helmholtz problem with different scaling functions. The goal is to receive sufficiently damped solutions.

The sketch in Figure (4.1) shows the propagation of the real part of a wave in 1D, i.e. the solution of a Helmholtz-type problem with an initial value with compact support in Ω_{int}. After a few time steps the wave moves in the directions of the boundaries of Ω_{int}, where the PML Ω_{pml} begins. At the interface the real part of the wave should be damped due to the scaling and decrease exponentially, such that no energy is reflected from the outer boundary of Ω_{pml}. Without the PML the waves move on towards the outer boundaries where they are reflected and proceed back into the inner domain.

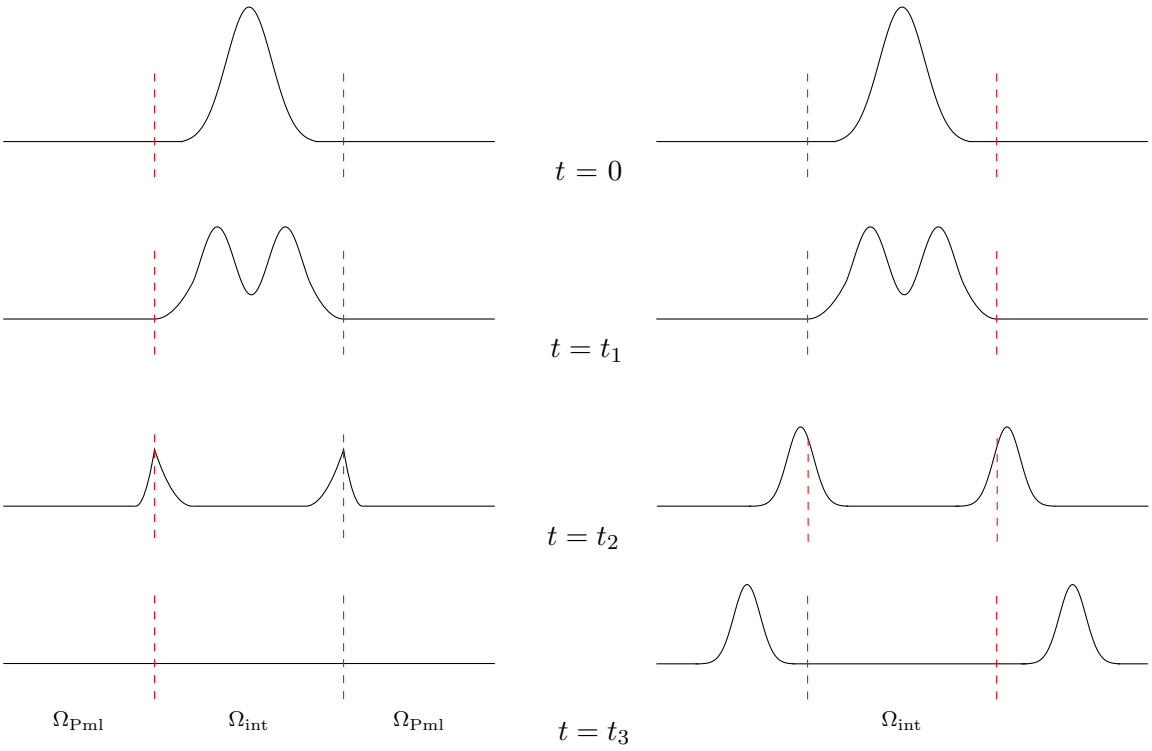

Figure 4.1: Propagation of waves with (left) and without (right) PMLs

4.3 Vertical scaling

We consider the vertical scaling function,

$$\sigma_1(\omega) = \begin{cases} 1, & x \in \Omega_{\text{int}}, \\ -\frac{\alpha}{i\omega}, & x \in \Omega_{\text{pml}}, \end{cases}$$

with $\alpha \in \mathbb{R}$, and examine its influence on the Klein-Gordon equation from system (4.3) in the variational formulation. Moreover, we define the function $\text{pot}(x)$ as a piecewise constant function with support in Ω_{pml}. This way it acts as a potential change. The following illustration explains why we call this the vertical scaling.

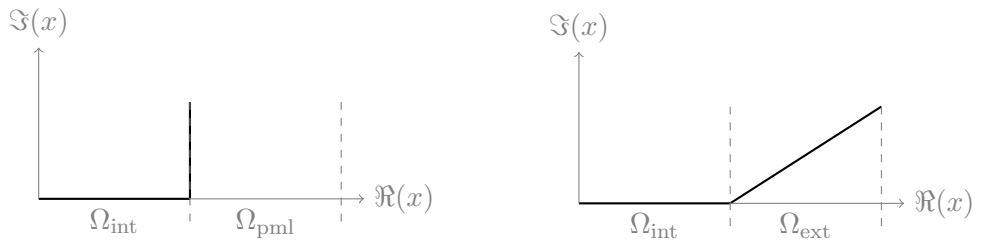

Figure 4.2: Scaling function $\sigma_1(\omega)$ on the left, and scaling $\sigma_2(\omega)$ (4.4) on the right side.

First, we multiply the terms with a test function $\tilde{p}$, integrate over the domain $\Omega = \Omega_{\text{int}} \cup \Omega_{\text{pml}}$ and use partial integration on the Laplacian term. Remembering that the variational formulation is not altered in Ω_{int} by the scaling function, we now only consider the changes within Ω_{pml}. Note that the potential function $\text{pot}(x)$ is constant in Ω_{pml}, and we can thus omit the dependence on x,

$$(-i\omega)^2 \int_{\Omega_{\text{pml}}} \frac{1}{c^2}\hat{p}(x)\tilde{p}(x)\ \mathrm{d}x + \int_{\Omega_{\text{pml}}} \partial_x\hat{p}(x)\partial_x\tilde{p}(x)\ \mathrm{d}x + \int_{\Omega_{\text{pml}}} \text{pot}^2\hat{p}(x)\tilde{p}(x)\ \mathrm{d}x = 0. \quad (4.8)$$

Corresponding to the bilinear forms (2.1) we define the following bilinear forms for $f, g \in H^1(\Omega)$

$$c_{\text{int}}(f,g) := \int_{\Omega_{\text{int}}} \text{pot}^2 f(x)g(x)\ \mathrm{d}x,$$
$$c_{\text{ext}}(f,g) := \int_{\Omega_{\text{ext}}} \text{pot}^2 f(x)g(x)\det J_\gamma(x)\ \mathrm{d}x.$$

The weak formulation of the Klein-Gordon problem is now stated as:

Problem 4.1. For a fixed $\omega > 0$ find $\hat{p} \in H^1(\Omega)$, such that

$$c^2 b_{\text{int}}(\hat{p},\tilde{p}) + c^2 b_{\text{ext}}(\hat{p},\tilde{p}) + c_{\text{int}}(\hat{p},\tilde{p}) + c_{\text{ext}}(\hat{p},\tilde{p}) = \omega^2(a_{\text{int}}(\hat{p},\tilde{p}) + a_{\text{ext}}(\hat{p},\tilde{p})),$$

for all test functions $\tilde{p} \in H^1\Omega$.

In the following we only consider the exterior bilinear forms. Next, the scaling function is applied to the spatial variable x, such that we can again denote the scaled variable as $\gamma(x) = \sigma(\omega)x$. Note that the scaling function $\sigma(\omega)$ contains the factor $-i\omega$, which, after transforming back from the frequency space, translates to a derivative in the time variable:

$$-\frac{\alpha}{i\omega} \quad \longleftrightarrow \quad \frac{\alpha}{\partial_t}.$$

Taking each integral of (4.8) and applying the scaling function to the spatial variable leads to a number of new integrals, corresponding to 2.1. We thus set

$$\begin{aligned} a_{\text{ext}}(\hat{p},\tilde{p}) &= (-i\omega)^2 \int_{\Omega_{\text{ext}}} \frac{1}{c^2}\hat{p}(x)\frac{\alpha}{-i\omega}\tilde{p}(x)\ \mathrm{d}x \\ &= -i\omega \int_{\Omega_{\text{ext}}} \frac{\alpha}{c^2}\hat{p}(x)\tilde{p}(x)\ \mathrm{d}x, \\ b_{\text{ext}}(\hat{p},\tilde{p}) &= \int_{\Omega_{\text{ext}}} \frac{-i\omega}{\alpha}\partial_x\hat{p}(x)\cdot\frac{-i\omega}{\alpha}\frac{\alpha}{-i\omega}\partial_x\tilde{p}(x)\ \mathrm{d}x \\ &= -i\omega \int_{\Omega_{\text{ext}}} \frac{1}{\alpha}\partial_x\hat{p}(x)\cdot\partial_x\tilde{p}(x)\ \mathrm{d}x. \end{aligned}$$

Defining the help function $v := \dfrac{\text{pot}\ \alpha}{-i\omega}\hat{p}$, the third term can be written as

$$\begin{aligned} c_{\text{ext}}(\hat{p},\tilde{p}) &= \int_{\Omega_{\text{ext}}} \text{pot}^2\hat{p}(x)\frac{\alpha}{-i\omega}\tilde{p}(x)\ \mathrm{d}x \\ &= \int_{\Omega_{\text{ext}}} \text{pot}\ \alpha v(x)\tilde{p}(x)\ \mathrm{d}x. \end{aligned}$$

The help function v and its test function w therefore have to satisfy the following equation:

$$i\omega \int_{\Omega_{\text{ext}}} v(x)w(x)\ \mathrm{d}x + \int_{\Omega_{\text{ext}}} \text{pot}\ \alpha p(x)w(x)\ \mathrm{d}x = 0. \tag{4.9}$$

The help function v is introduced to dispose of the fraction in $-i\omega$.

The implementation is done in *Netgen/NGSolve*, where one can easily define compound finite element spaces with trial functions from different spaces:

```
h1 = H1(mesh,order=order,complex=False)
h1pml = H1(mesh,order=order,definedon=mesh.Materials('pml'),complex=False)
l2pml = L2(mesh,order=order-1,definedon=mesh.Materials('pml'),complex=False)
fes = FESpace([h1,l2pml])

p,v = fes.TrialFunction()
q,w = fes.TestFunction()
```

In the code snippet above we define `fes` as the compound finite element space with corresponding trial and test function pairs.

4.3.1 Helmholtz

The vertical scaling $\frac{\alpha}{-i\omega}$ performs well on the Helmholtz equation, but as is shown later it does not lead to a damped solution in the case of the Klein-Gordon equation. Applying $\sigma_1(\omega)$ to the solution yields:

$$\hat{p}(x) = \exp(i\sqrt{\omega^2}\sigma_1(\omega)x) = \exp(-\alpha x).$$

Hence, this scaling is optimal for $\alpha > 0$ and performs equally well for all ω, because the solution has exponential decay independent from the frequencys. For the Helmholtz problem it is thus primarily not necessary to consider additional scaling functions, which may lead to a larger system due to more needed help functions.

4.3.2 Klein-Gordon

The solution of the Klein-Gordon problem, however, can not be damped with $\sigma_1(\omega)$. First, we consider the case $\omega > \text{pot}$. We have

$$\sigma_1(\omega) i\sqrt{\omega^2 - \text{pot}^2} = -\alpha \underbrace{\frac{\sqrt{\omega^2 - \text{pot}^2}}{\omega}}_{>0},$$

which, integrated into the solution, yields

$$\hat{p}(x) = \exp\left(-\alpha \frac{\sqrt{\omega^2 - \text{pot}^2}}{\omega} x\right).$$

This leads to exponential decay for $\alpha > 0$. In the other case, if $\omega < \text{pot}$, the solution is

$$\hat{p}(x) = \exp\Big(- \sqrt{\text{pot}^2 - \omega^2}\Big(\frac{-\alpha}{i\omega}\Big)x\Big) = \exp\left(- i\alpha\frac{\sqrt{\text{pot}^2 - \omega^2}}{\omega}x\right)$$

and thus oscillates for $\alpha > 0$ and does not decay.

In the first case the solution is damped exponentially with $\alpha > 0$, but for small frequencies the solution oscillates and is not damped. Thus, other scaling functions better suited for this problem are further considered.

4.4 Diagonal scaling function

A different approach for a scaling function is (see Figure 4.2):

$$\sigma_2(\omega) = \begin{cases} 1, & x \in \Omega_{\text{int}}, \\ \dfrac{-\beta i\omega + \alpha}{-i\omega}, & x \in \Omega_{\text{pml}}, \end{cases}$$

with $\alpha, \beta \in \mathbb{R}$. Applying $\sigma_2(\omega)$ to (4.3), we get the integrals:

$$\begin{aligned} a_{\text{ext}}(\hat{p}, \tilde{p}) &= (-i\omega)^2 \int_{\Omega_{\text{ext}}} \frac{1}{c^2}\hat{p}(x)\tilde{p}(x)\left(\frac{\beta(-i\omega)+\alpha}{-i\omega}\right) \,\mathrm{d}x \\ &= (-i\omega)^2 \int_{\Omega_{\text{ext}}} \frac{\beta}{c^2}\hat{p}(x)\tilde{p}(x) \,\mathrm{d}x + (-i\omega)^2 \int_{\Omega_{\text{ext}}} \frac{\alpha}{c^2}\hat{p}(x)\frac{1}{-i\omega}\tilde{p}(x) \,\mathrm{d}x \end{aligned}$$

The second term reads as

$$\begin{aligned} b_{\text{ext}}(\hat{p}, \tilde{p}) &= \int_{\Omega_{\text{ext}}} \left(\frac{-i\omega}{\beta(-i\omega)+\alpha}\right) \partial_x\hat{p}(x) \left(\frac{-i\omega}{\beta(-i\omega)+\alpha}\right) \partial_x\tilde{p}(x) \left(\frac{\beta(-i\omega)+\alpha}{-i\omega}\right) \,\mathrm{d}x \\ &= \int_{\Omega_{\text{ext}}} \left(\frac{-i\omega}{\beta(-i\omega)+\alpha}\right) \partial_x\hat{p}(x)\partial_x\tilde{p}(x) \,\mathrm{d}x \\ &= -i\omega \int_{\Omega_{\text{ext}}} (-i\omega c_1 + c_2) g(x)\partial_x\tilde{p}(x) \,\mathrm{d}x \\ &= (-i\omega)^2 \int_{\Omega_{\text{ext}}} c_1 g(x)\partial_x\tilde{p}(x) \,\mathrm{d}x - i\omega \int_{\Omega_{\text{ext}}} c_2 g(x)\partial_x\tilde{p}(x) \,\mathrm{d}x, \end{aligned}$$

whereas the help function g is defined via $c_1(-i\omega)g + c_2 g = \dfrac{\partial_x\hat{p}}{\beta(-i\omega)+\alpha}$ with the corresponding test function z. Together the functions fulfill the following equation:

$$\begin{aligned} (-i\omega)^2 \int_{\Omega_{\text{ext}}} c_1\beta g(x)z(x) \,\mathrm{d}x - i\omega \int_{\Omega_{\text{ext}}} (c_2\beta + c_1\alpha) g(x)z(x) \,\mathrm{d}x \\ + \int_{\Omega_{\text{ext}}} c_2 g(x)z(x) \,\mathrm{d}x - \int_{\Omega_{\text{ext}}} \partial_x p(x)z(x) \,\mathrm{d}x = 0. \end{aligned}$$

The third term reads as

$$\begin{aligned} c_{\text{ext}}(\hat{p},\tilde{p}) &= \int_{\Omega_{\text{ext}}} \text{pot}^2\hat{p}(x)\tilde{p}(x)\left(\frac{\beta(-i\omega)+\alpha}{-i\omega}\right)\,\mathrm{d}x \\ &= \int_{\Omega_{\text{ext}}} \beta\text{pot}^2\hat{p}(x)\tilde{p}(x)\,\mathrm{d}x + \int_{\Omega_{\text{ext}}} \text{pot}^2\hat{p}(x)\tilde{p}(x)\frac{\alpha}{-i\omega}\,\mathrm{d}x \end{aligned}$$

With the additional help function v defined by the equation $\partial_t c_3 v + c_4 v = \dfrac{\text{pot}\ \alpha}{-i\omega}p$ and its corresponding test function w, the third term now reads:

$$\begin{aligned} \int_{\Omega_{\text{ext}}} \text{pot}^2\hat{p}(x)\tilde{p}(x)\,\mathrm{d}\hat{x} &= \int_{\Omega_{\text{ext}}} \text{pot}^2\hat{p}(x)\tilde{p}(x)\left(\frac{\beta(-i\omega)+\alpha}{-i\omega}\right)\,\mathrm{d}x \\ &= \int_{\Omega_{\text{ext}}} \beta\text{pot}^2\hat{p}(x)\tilde{p}(x)\,\mathrm{d}x + \int_{\Omega_{\text{ext}}} \text{pot}(-i\omega c_3 v(x) + c_4 v(x))\tilde{p}(x)\,\mathrm{d}x \\ &= \int_{\Omega_{\text{ext}}} \beta\text{pot}^2\hat{p}(x)\tilde{p}(x)\,\mathrm{d}x - i\omega\int_{\Omega_{\text{ext}}} c_3\text{pot}v(x)\tilde{p}(x)\,\mathrm{d}x \\ &\quad + \int_{\Omega_{\text{ext}}} c_4\text{pot}v(x)\tilde{p}(x)\,\mathrm{d}x, \end{aligned}$$

whereas the help function v has to fulfill

$$(-i\omega)^2\int_{\Omega_{\text{ext}}} c_3 v(x)w(x)\,\mathrm{d}x - i\omega\int_{\Omega_{\text{ext}}} c_4 v(x)w(x)\,\mathrm{d}x = \int_{\Omega_{\text{ext}}} \text{pot}\alpha\hat{p}(x)w(x)\,\mathrm{d}x.$$

Hence, the problem contains three trial functions: the solution p, and the help functions v and g, leading to a larger system matrix than in the case above.

4.4.1 Helmholtz

In the case of $\sigma_2(\omega)$ we have $i\omega\sigma_2(\omega) = i\omega\left(\beta - \frac{\alpha}{i\omega}\right) = \beta i\omega - \alpha$. The real part of the solution of the Helmholtz equation,

$$\begin{aligned} \hat{p}(x) = \exp(i\omega\sigma_2(\omega)x) &= \exp(\beta i\omega x - \alpha x) \\ &= \exp(-\alpha x)(\cos(\beta\omega x) + i\sin(\beta\omega x)), \end{aligned}$$

is thus decreasing exponentially with $\alpha > 0$ and $\beta \in \mathbb{R}$. The exponential decay is not dependent on ω, but the oscillation is.

4.4.2 Klein-Gordon

If $\omega > \text{pot}$, the scaled solution of the Klein-Gordon equation takes the form

$$\begin{aligned} \hat{p}(x) &= \exp\left(i\sqrt{\omega^2-\text{pot}^2}\left(\beta - \frac{\alpha}{i\omega}\right)x\right) = \\ &= \exp\left(i\beta\sqrt{\omega^2-\text{pot}^2}x - \alpha\frac{\sqrt{\omega^2-\text{pot}^2}}{\omega}x\right) \\ &= \exp\left(-\alpha\frac{\sqrt{\omega^2-\text{pot}^2}}{\omega}x\right)\left(\cos\left(\beta\sqrt{\omega^2-\text{pot}^2}x\right) + i\sin\left(\beta\sqrt{\omega^2-\text{pot}^2}x\right)\right), \end{aligned} \tag{4.10}$$

and the solution has exponential decay for $\alpha > 0$ and $\beta \in \mathbb{R}$.

For $\omega < \text{pot}$, the solution is

$$\hat{p}(x) = \exp\left(-\beta\sqrt{\text{pot}^2 - \omega^2}x + i\alpha\frac{\sqrt{\text{pot}^2 - \omega^2}}{\omega}x\right),$$

and the solution thus decreases for $\beta > 0$ and $\alpha \in \mathbb{R}$.

Again, considering (4.10) we observe for high frequencies, using the result

$$\lim_{\omega\to\infty}\frac{\sqrt{\omega^2 - \text{pot}^2}}{\omega} = 1,$$

that the exponential decay is not dependent on ω and the solution converges to 0 for $x \to \infty$. Again, the exponential decay is not dependent on ω, but the oscillation is.

4.5 Convolutional scaling

The third considered scaling function is the so-called convolutional scaling:

$$\sigma_3(\omega) = \begin{cases} 1, & x \in \Omega_{\text{int}}, \\ \alpha_1 + \dfrac{\alpha_2 + \frac{\alpha_3}{-i\omega}}{\beta_1 - \beta_2 i\omega}, & x \in \Omega_{\text{pml}}, \end{cases}$$

for $\alpha_1, \alpha_2, \alpha_3, \beta_1, \beta_2 \in \mathbb{R}$. We make the specification $\alpha_1 = 0$, as we later see from the explicit solution that this additional parameter deteriorates the decay of the solutions of the Helmholtz and the Klein-Gordon problems.

First, rewrite the scaling function in the following way:

$$\frac{\alpha_2 + \frac{\alpha_3}{-i\omega}}{\beta_1 - \beta_2 i\omega} = \frac{\alpha_2 i\omega - \alpha_3}{\beta_1 i\omega - \beta_2(-i\omega)^2}.$$

The first term of (4.3) thus reads

$$\begin{aligned} a_{\text{ext}}(\hat{p}, \tilde{p}) &= (-i\omega)^2 \int_{\Omega_{\text{ext}}} \frac{\alpha_2}{\beta_1 + \beta_2(-i\omega)}\hat{p}(x)\tilde{p}(x)\,\mathrm{d}x \\ &= (-i\omega)^2 \int_{\Omega_{\text{ext}}} \alpha_2 g(x)\tilde{p}(x)\,\mathrm{d}x - (-i\omega)^2 \int_{\Omega_{\text{ext}}} \alpha_3 v(x)\tilde{p}(x)\,\mathrm{d}x, \end{aligned}$$

whereas we have introduced two new help and corresponding test functions functions (g, z) and (v, w) defined via $g := \dfrac{1}{\beta_1 + \beta_2(-i\omega)}p$ and $v := \dfrac{1}{-\beta_1(-i\omega) - \beta_2(-i\omega)^2}p$ fulfilling

$$\int_{\Omega_{\text{ext}}} \beta_1 g(x)z(x)\,\mathrm{d}x - i\omega\int_{\Omega_{\text{ext}}} \beta_2 g(x)z(x)\,\mathrm{d}x - \int_{\Omega_{\text{ext}}} p(x)z(x)\,\mathrm{d}x = 0,$$

and

$$i\omega \int_{\Omega_{\text{ext}}} \beta_1 v(x)w(x)\ \mathrm{d}x - (-i\omega)^2 \int_{\Omega_{\text{ext}}} \beta_2 v(x)w(x)\ \mathrm{d}x - \int_{\Omega_{\text{ext}}} p(x)w(x)\ \mathrm{d}x = 0.$$

The second term reformulates to

$$\begin{aligned} b_{\text{ext}}(\hat{p},\tilde{p}) &= i\omega \int_{\Omega_{\text{ext}}} \frac{\beta_1}{-\alpha_2(-i\omega)-\alpha_3} \partial_x\hat{p}(x)\partial_x\tilde{p}(x)\ \mathrm{d}x \\ &\quad - (-i\omega)^2 \int_{\Omega_{\text{ext}}} \frac{\beta_2}{-\alpha_2(-i\omega)-\alpha_3} \partial_x\hat{p}(x)\partial_x\tilde{p}(x)\ \mathrm{d}x \\ &= i\omega \int_{\Omega_{\text{ext}}} \beta_1 s\partial_x\tilde{p}(x)\ \mathrm{d}x - (-i\omega)^2 \int_{\Omega_{\text{ext}}} \beta_2 s\partial_x\tilde{p}(x)\ \mathrm{d}x, \end{aligned}$$

using the help function $s := \dfrac{1}{-\alpha_2(-i\omega)-\alpha_3}\partial_x\hat{p}$ with corresponding test function r fulfilling

$$i\omega \int_{\Omega_{\text{ext}}} \alpha_2 s(x)r(x)\ \mathrm{d}x - \int_{\Omega_{\text{ext}}} \alpha_3 s(x)r(x)\ \mathrm{d}x - \int_{\Omega_{\text{ext}}} \partial_x\hat{p}(x)r(x)\ \mathrm{d}x = 0.$$

The third term now reads

$$c_{\text{ext}}(\hat{p},\tilde{p}) = \int_{\Omega_{\text{ext}}} \text{pot}^2\alpha_2 g(x)\tilde{p}(x)\ \mathrm{d}x - \int_{\Omega_{\text{ext}}} \text{pot}^2\alpha_3 v(x)\tilde{p}(x)\ \mathrm{d}x.$$

Hence, we need three additional test functions.

4.5.1 Helmholtz

For the convolutional scaling we calculate

$$\begin{aligned} i\omega\sigma_3(\omega) &= \frac{\alpha_2 i\omega - \alpha_3}{\beta_1 - \beta_2 i\omega} \\ &= \frac{-\alpha_3\beta_1 - \alpha_2\beta_2\omega^2}{\beta_1^2+\beta_2^2\omega^2} + i\frac{\alpha_2\beta_1\omega - \alpha_3\beta_2\omega}{\beta_1^2+\beta_2^2\omega^2}. \end{aligned}$$

Integrating this into the solution yields

$$\hat{p}(x) = \exp\left(\frac{-\alpha_3\beta_1 - \alpha_2\beta_2\omega^2}{\beta_1^2+\beta_2^2\omega^2}x\right)\left(\cos\left(\frac{\alpha_2\beta_1\omega - \alpha_3\beta_2\omega}{\beta_1^2+\beta_2^2\omega^2}x\right) + i\sin\left(\frac{\alpha_2\beta_1\omega - \alpha_3\beta_2\omega}{\beta_1^2+\beta_2^2\omega^2}x\right)\right).$$

The solution thus has exponential decay if $\alpha_2, \alpha_3, \beta_1, \beta_2 > 0$.

For high frequencies we observe

$$\lim_{\omega\to\infty} \frac{-\alpha_3\beta_1 - \alpha_2\beta_2\omega^2}{\beta_1^2+\beta_2^2\omega^2} = -\frac{\alpha_2}{\beta_2}, \qquad \lim_{\omega\to\infty} \frac{\alpha_2\beta_1\omega - \alpha_3\beta_2\omega}{\beta_1^2+\beta_2^2\omega^2} = 0,$$

such that the decay and the oscillations become independent from ω.

The additional parameter α_1 mentioned above would increase the oscillations and is therefore omitted. For the diagonal scaling, however, it is useful.

We observe that the vertical scaling function $\sigma_1(\omega)$ is a special case of $\sigma_3(\omega)$ if we set $\alpha_2 = 0, \alpha_3 = \alpha, \beta_1 = 1$, and $\beta_2 = 0$. Also, the diagonal scaling $\sigma_2(\omega)$ is a special case of $\sigma_3(\omega)$ if we set $\alpha_1 = \beta, \alpha_2 = 0, \alpha_3 = \alpha, \beta_1 = 1$, and $\beta_2 = 0$.

4.5.2 Klein-Gordon

Again, we start by considering the case $\omega > \text{pot}$, such that we have for the solution

$$\begin{aligned}\hat{p}(x) &= \exp\left(i\frac{\alpha_3 - \alpha_2 i\omega}{\beta_1 i\omega + \beta_2\omega^2}\sqrt{\omega^2 - \text{pot}^2}x\right) \\ &= \exp\left(-\frac{\alpha_3\beta_1 + \alpha_2\beta_2\omega^2}{\beta_1^2 + \beta_2^2\omega^2}\frac{\sqrt{\omega^2 - \text{pot}^2}}{\omega}x\right)\left(\cos\left(\frac{\alpha_2\beta_1 - \alpha_3\beta_2}{\beta_1^2 + \beta_2^2\omega^2}\sqrt{\omega^2 - \text{pot}^2}x\right)\right. \\ &\qquad \left. + i\sin\left(\frac{\alpha_2\beta_1 - \alpha_3\beta_2}{\beta_1^2 + \beta_2^2\omega^2}\sqrt{\omega^2 - \text{pot}^2}x\right)\right),\end{aligned}$$

and the solution has exponential decay if $\alpha_2, \alpha_3, \beta_1, \beta_2 > 0$.
If $\omega < \text{pot}$ the solution yields

$$\begin{aligned}\hat{p}(x) &= \exp\left(\frac{\alpha_3 - \alpha_2 i\omega}{\beta_1 i\omega + \beta_2\omega^2}\sqrt{\text{pot}^2 - \omega^2}x\right) \\ &= \exp\left(\frac{\alpha_3\beta_2 - \alpha_2\beta_1}{\beta_1^2 + \beta_2^2\omega^2}\sqrt{\text{pot}^2 - \omega^2}x\right)\left(\cos\left(-\frac{\alpha_2\beta_2\omega^2 + \alpha_3\beta_1}{\beta_1^2\omega + \beta_2^2\omega^3}\sqrt{\text{pot}^2 - \omega^2}x\right)\right. \\ &\qquad \left. + i\sin\left(-\frac{\alpha_2\beta_2\omega^2 + \alpha_3\beta_1}{\beta_1^2\omega + \beta_2^2\omega^3}\sqrt{\text{pot}^2 - \omega^2}x\right)\right).\end{aligned}$$

Thus, we need to ensure that $\alpha_3\beta_2 - \alpha_2\beta_1 > 0$ for $\alpha_2, \alpha_3, \beta_1, \beta_2 > 0$ for the solution to have exponential decay.

For high frequencies we observe

$$\lim_{\omega\to\infty} -\frac{\alpha_3\beta_1 + \alpha_2\beta_2\omega^2}{\beta_1^2 + \beta_2^2\omega^2}\frac{\sqrt{\omega^2 - \text{pot}^2}}{\omega} = -\frac{\alpha_2}{\beta_2}.$$

and we find that the exponential decay is independent from ω. The oscillations also become independent from ω as we observe

$$\lim_{\omega\to\infty} \frac{\alpha_2\beta_1 - \alpha_3\beta_2}{\beta_1^2 + \beta_2^2\omega^2}\sqrt{\omega^2 - \text{pot}^2} = 0.$$

4.6 Comparing the scaling functions

The question arises why different scaling functions are considered and for which examples they are appropriate. In this section we want to argue why in special cases it makes more sense to use the second (4.4) or the convolutional scaling (4.5) instead of the vertical scaling (4.3) even though the variational formulations become more complex and more help functions have to be introduced, which further enlarges the system matrix.

In Example 1 the vertical scaling is applied to the Helmholtz problem, and in the second example we show how the vertical scaling fails to damp the solution of the Klein-Gordon problem. In the third example we consider a problem to argue for which settings the convolutional scaling performs better than the diagonal scaling.

All implementations and plots are done within the Python interface *NGS-Py* of the finite element software *Netgen/NGSolve*[1], which includes a mesh generator (see [Sch97],[Sch14]).

Since we already rewrote the problems as second order systems in time, we use the second order time integration method from Section (3.5).

[1] https://ngsolve.org/

4.6.1 Example 1

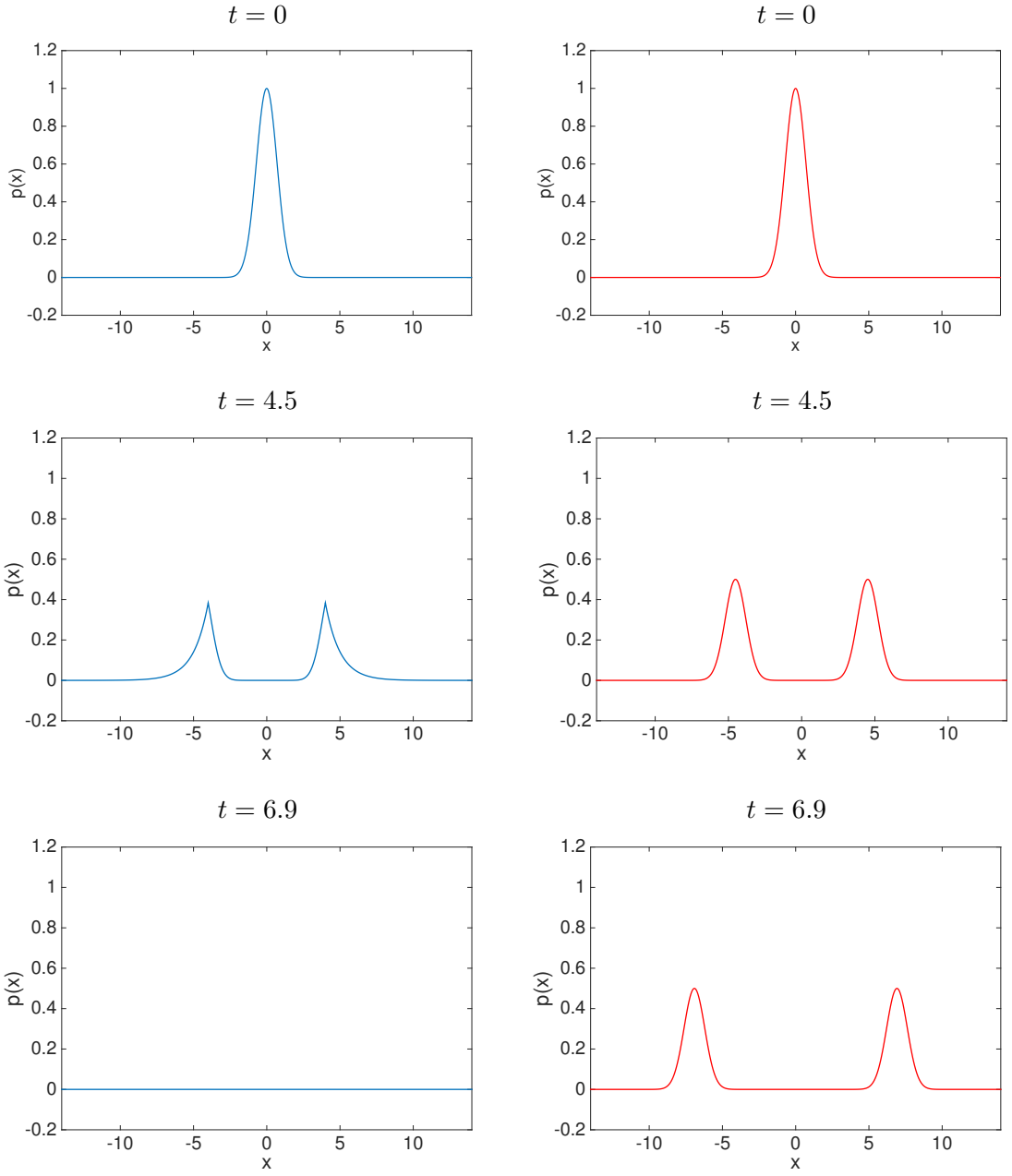

Figure 4.3: Solution of Helmholtz problem with scaling $\sigma_1(\omega)$ and PML layers $[-14, 4]$ and $[4, 14]$ on the left (blue) and without PML on the right (red).

Figure 4.1 has already shown us how the solution of the Helmholtz problem should behave when using the PML method. If we set pot $\equiv 0$ in the considerations from above, we effectively solve the Helmholtz problem, and the solution should be damped well for all scaling functions.

In Figure 4.3 the solution of the following example using the scaling function $\sigma_1(\omega)$ is shown. In this example we consider $\Omega_{\text{int}} = [-4, 4]$ and a PML of thickness 10. The initial condition is a gaussian peak. The outgoing wave is damped in Ω_{pml} according to the considerations from before. Without any scaling the wave proceeds to move outside of Ω_{int} and is eventually reflected at the outer boundary. The other scaling functions transport the energy outside of Ω_{int} in the same manner.

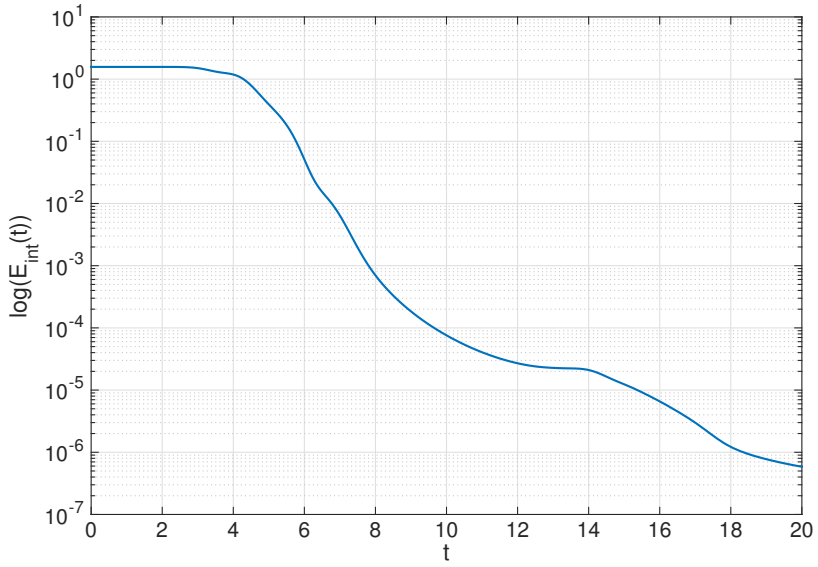

Figure 4.4: Energy over time in inner domain Ω_{int}

Figure 4.4 shows the Energy in the inner domain of the complex scaled solution,

$$E(p) = \frac{1}{2} \int_{\Omega_{\text{int}}} (|p_t(t,x)|^2 + |\partial_x p(t,x)|^2) \, \mathrm{d}x.$$

A plateau is visible at the beginning, where the wave has not left the domain. After surpassing the interface, the PML starts and the solution is damped, such that no energy proceeds back into Ω_{int}.

4.6.2 Example 2

The vertical scaling function (4.3) works fine for the Helmholtz equation with either an initial condition with support in Ω_{int}. In this case it is thus not necessary to define other, more expensive, scalings. However, the Klein-Gordon equation shows different results due to the potential term (pot) indicating a difference in material.

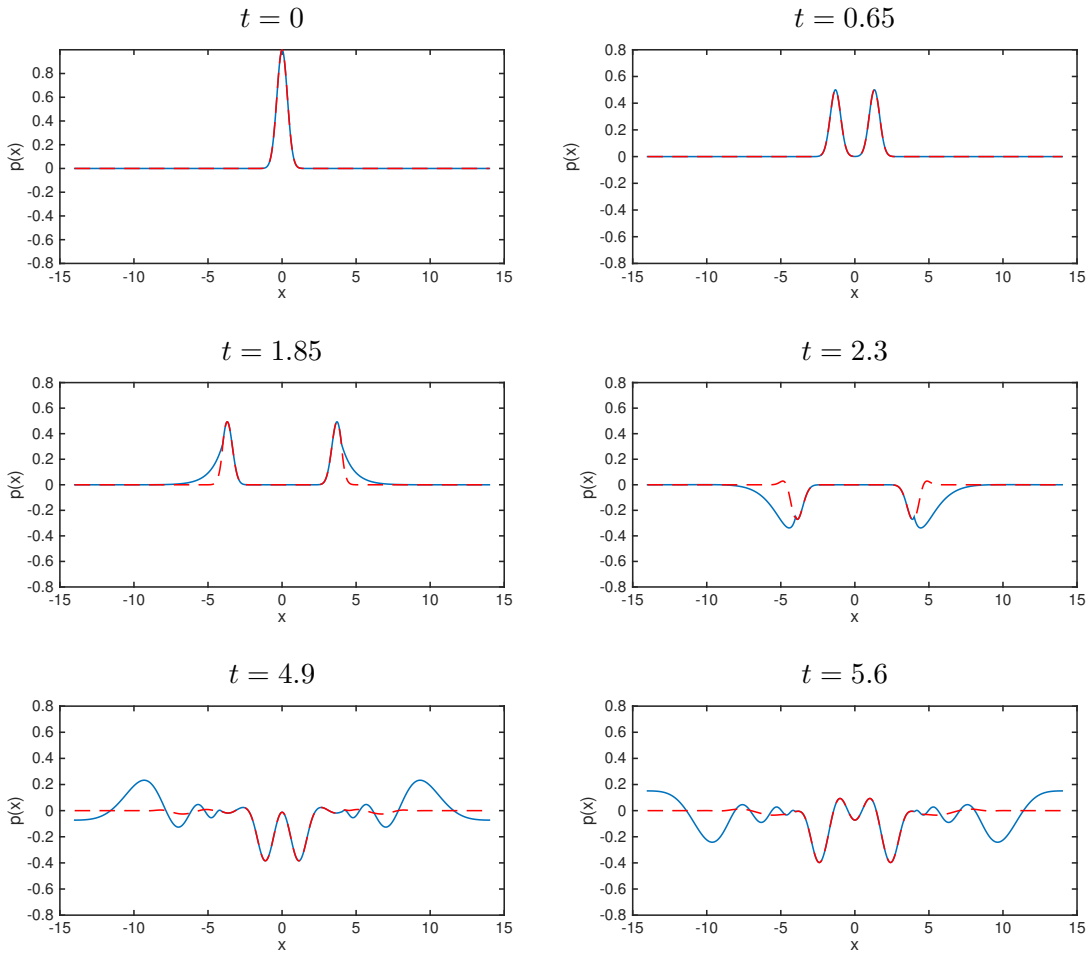

Figure 4.5: Comparison of scaling functions (blue: $\sigma_1(\omega) = -\frac{\alpha}{i\omega}$, red dashed: $\sigma_3(\omega) = \beta - \frac{\alpha}{i\omega}$) for Klein-Gordon equation with potential at interface (-4 and 4).

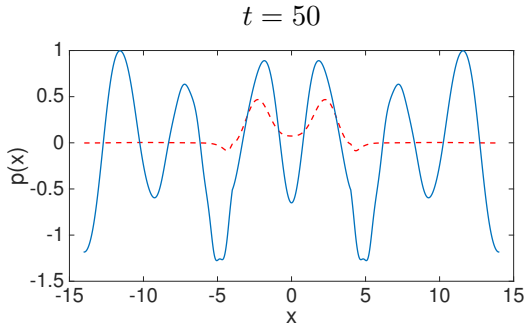

Figure 4.6: Solution at time $t = 50$ with $\sigma_1(\omega)$ (blue) and $\sigma_3(\omega)$ (red dashed).

Figure 4.5 represents the solution of the Klein Gordon equation with a potential

$$\mathrm{pot}(x) = \begin{cases} 0 & x \in \Omega_{\mathrm{int}}, \\ 3 & x \in \Omega_{\mathrm{pml}}, \end{cases}$$

and a gaussian peak in the origin as initial value at different time steps. The inner domain was set as $\Omega_{\mathrm{int}} = [-4, 4]$. The PMLs on the left and right side are $[-14, -4]$, and $[4, 14]$ and are as such considerably large. This was done to eliminate the suspicion of reflections due to too early truncation. The time step was set as $\tau = 0.01$. The blue line represents the solution with the vertical scaling, and the red dashed line shows the solution with the convolutional scaling. For this scaling the solution is not well damped in the PMLs, whereas the convolutional scaling σ_3 manages to absorb the solution, which is the desired property of the PML method. Note that the diagonal scaling σ_2 also works for this problem. At time step $t = 1.85$ the moment is captured where the outgoing wave starts to surpass the interface. The later snapshots show that the solution with the vertical scaling does not stay near zero, and even alternates in a wide range between positive and negative values. As time passes, energy proceeds back into Ω_{int} when using the vertical scaling $\sigma_1(\omega)$, thus distorting the solution in the interior. This can be seen in Figure 4.6. The convolutional scaling manages to damp the solution at the boundary.

4.6.3 Example 3

This example shows a case in which the convolutional scaling performs better than the diagonal scaling. The inner domain was set as $[-1.5, 1.5]$ with PMLs of thickness 10 on both sides. We choose an initial value that produces high oscillations,

$$r(x) := \begin{cases} 0, & x < -1, \\ \sin(50x), & x \in [-1, 1], \\ 0, & x > 1. \end{cases}$$

Figure 4.7 shows the solution with the convolutional scaling (red dashed) and the diagonal scaling (blue), whereas the solutions are overlapping in Ω_{int}. The wave packs proceed towards the interface.

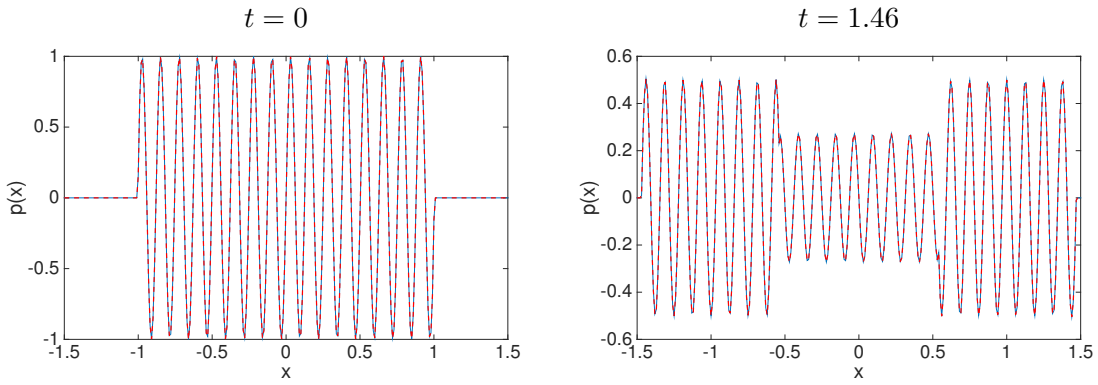

Figure 4.7: Solution with initial source $r(x)$ in Ω_{int}.

Figure 4.8 shows the solution after the waves have reached the PMLs. The solutions are zero at the outer boundary of the PMLs for both scalings, and zooming in on the left plot we can see in the right plot that both solutions have exponential decay. However, the solution with the diagonal scaling $\sigma_2(\omega)$ (blue) shows high oscillations in the PML region. The solution with the convolutional scaling $\sigma_3(\omega)$ (red dashed) is much smoother, and we can therefore argue that the spatial discretization in the PML region must be much finer when using the diagonal scaling adding to computational costs.

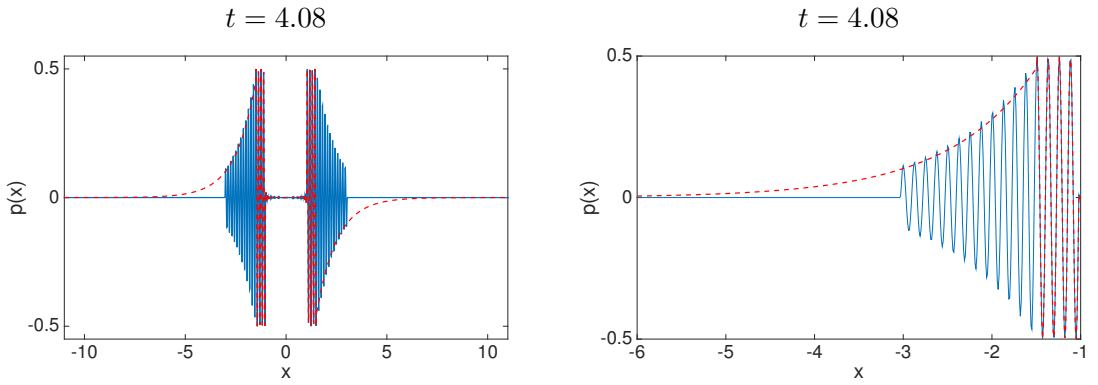

Figure 4.8: Damping of the solution with convolutional scaling $\sigma_3(\omega)$ (red dashed) and diagonal scaling $\sigma_2(\omega)$ (blue).

The H^1-seminorm in the PML domain is defined as

$$|p|_{H^1(\Omega_{\text{pml}})} := ||\partial_x p||_{L_2(\Omega_{\text{pml}})} = \left(\int_{\Omega_{\text{pml}}} \partial_x p(x,t) \cdot \partial_x p(x,t) \, \mathrm{d}x \right)^{\frac{1}{2}},$$

and is shown in Figure 4.9.

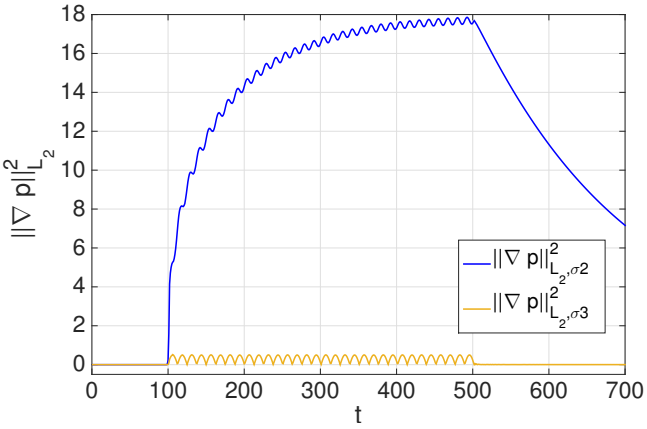

Figure 4.9: H(t) over time for the convolutional scaling (red) and the diagonal scaling (blue) in Ω_{pml}.

At $t = 100$ the wave pack arrives at the interface. For the diagonal scaling the H^1-seminorm keeps growing until all the energy has left the inner domain, and only then it starts decreasing.

5 Curvilinear complex scaling in 2D

As discussed before, the starting point for the complex scaling with curvilinear coordinates is the system (2.23):

$$\begin{aligned}\int_{\mathbb{R}_+\times\Gamma} \frac{\partial\hat{p}}{\partial\xi}\frac{\partial\tilde{p}}{\partial\xi}\frac{1+\kappa\sigma(\omega)\xi}{\sigma(\omega)}\,\mathrm{d}(\xi,\hat{\mathbf{x}}) + i\omega\int_{\mathbb{R}_+\times\Gamma}\sigma(\omega)u\nabla_\Gamma\tilde{p}\cdot\tau\,\mathrm{d}(\xi,\hat{\mathbf{x}})\\ +(-i\omega)^2\int_{\mathbb{R}_+\times\Gamma}\sigma(\omega)(1+\kappa\sigma(\omega)\xi)\hat{p}\tilde{p}\,\mathrm{d}(\xi,\hat{\mathbf{x}}) = 0, \qquad (5.1)\\ (-i\omega)^2\int_{\mathbb{R}_+\times\Gamma}(1+\kappa\sigma(\omega)\xi)u\tilde{u}\sigma(\omega)\,\mathrm{d}(\xi,\hat{\mathbf{x}}) + i\omega\int_{\mathbb{R}_+\times\Gamma}\nabla_\Gamma\hat{p}\cdot\tau\tilde{u}\sigma(\omega)\,\mathrm{d}(\xi,\hat{\mathbf{x}}) = 0.\end{aligned}$$

This system is written with wave speed $\equiv 1$, but we want to consider a formulation with wave speed $c(x)$ that is constant inside and outside of the wave guide as illustrated in Figure 5.1. Outside of Ω_{int} it is defined as

$$c|_{\Omega_{\text{ext}}}(x) = \hat{c}(\hat{\mathbf{x}}(x)).$$

The mass term in (5.1) is thus multiplied with $1/c^2(x)$.

We consider this problem on open waveguides as shown in Figure 5.1. Using this geometry we are not able to use cartesian or radial coordinates, since the inhomogeneity in the exterior does not align with these coordinates.

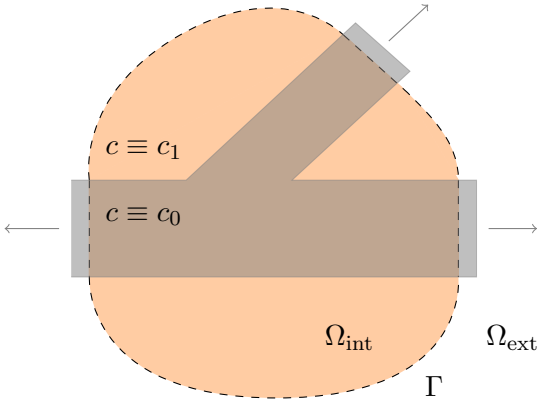

Figure 5.1: Open waveguide.

We define the following bilinear forms

$$
\begin{aligned}
a(\begin{pmatrix}\hat{p}\\ u\end{pmatrix},\begin{pmatrix}\tilde{p}\\ \tilde{u}\end{pmatrix}) &:= \int_{\mathbb{R}_+\times\Gamma} \frac{\partial\hat{p}}{\partial\xi}\frac{\partial\tilde{p}}{\partial\xi}\ \mathrm{d}(\xi,\hat{\mathbf{x}}),\\
b(\begin{pmatrix}\hat{p}\\ u\end{pmatrix},\begin{pmatrix}\tilde{p}\\ \tilde{u}\end{pmatrix}) &:= \int_{\mathbb{R}_+\times\Gamma} \frac{\partial\hat{p}}{\partial\xi}\frac{\partial\tilde{p}}{\kappa}\xi\partial\xi\ \mathrm{d}(\xi,\hat{\mathbf{x}}) + \int_{\Omega_{\mathrm{int}}} \nabla\hat{p}\cdot\nabla\tilde{p}(\xi,\hat{\mathbf{x}}),\\
c(\begin{pmatrix}\hat{p}\\ u\end{pmatrix},\begin{pmatrix}\tilde{p}\\ \tilde{u}\end{pmatrix}) &:= -\int_{\mathbb{R}_+\times\Gamma} (u\nabla_\Gamma\tilde{p}\cdot\tau + \nabla_\Gamma\hat{p}\cdot\tau\tilde{u})\ \mathrm{d}(\xi,\hat{\mathbf{x}}),\\
d(\begin{pmatrix}\hat{p}\\ u\end{pmatrix},\begin{pmatrix}\tilde{p}\\ \tilde{u}\end{pmatrix}) &:= \int_{\mathbb{R}_+\times\Gamma} \left(\frac{1}{c^2}\hat{p}\tilde{p} - u\cdot\tilde{u}\right)\ \mathrm{d}(\xi,\hat{\mathbf{x}}),\\
e(\begin{pmatrix}\hat{p}\\ u\end{pmatrix},\begin{pmatrix}\tilde{p}\\ \tilde{u}\end{pmatrix}) &:= \int_{\mathbb{R}_+\times\Gamma} \left(\frac{1}{c^2}\hat{p}\tilde{p} - u\cdot\tilde{u}\right)\kappa\xi\ \mathrm{d}(\xi,\hat{\mathbf{x}}),\\
f(\begin{pmatrix}\hat{p}\\ u\end{pmatrix},\begin{pmatrix}\tilde{p}\\ \tilde{u}\end{pmatrix}) &:= \int_{\Omega_{\mathrm{int}}} \frac{1}{c^2}\hat{p}\tilde{p}\ \mathrm{d}(\xi,\hat{\mathbf{x}}),
\end{aligned}
$$

and can rewrite the system (2.23) as

$$
\begin{aligned}
\frac{1}{\sigma(\omega)}a(\begin{pmatrix}\hat{p}\\ u\end{pmatrix},\begin{pmatrix}\tilde{p}\\ \tilde{u}\end{pmatrix}) + b(\begin{pmatrix}\hat{p}\\ u\end{pmatrix},\begin{pmatrix}\tilde{p}\\ \tilde{u}\end{pmatrix}) + (-i\omega)\sigma(\omega)c(\begin{pmatrix}\hat{p}\\ u\end{pmatrix},\begin{pmatrix}\tilde{p}\\ \tilde{u}\end{pmatrix}) + (-i\omega)^2\sigma(\omega)d(\begin{pmatrix}\hat{p}\\ u\end{pmatrix},\begin{pmatrix}\tilde{p}\\ \tilde{u}\end{pmatrix})\\
+(-i\omega)^2\sigma(\omega)^2e(\begin{pmatrix}\hat{p}\\ u\end{pmatrix},\begin{pmatrix}\tilde{p}\\ \tilde{u}\end{pmatrix}) + (-i\omega)^2f(\begin{pmatrix}\hat{p}\\ u\end{pmatrix},\begin{pmatrix}\tilde{p}\\ \tilde{u}\end{pmatrix}) = 0.
\end{aligned}
$$

Discretization yields matrices A, B, C, D, E, F for the bilinear forms a, b, c, d, e, f. A right-hand side can be introduced in the same way. The discretized system reads as

$$
\left(\frac{1}{\sigma(\omega)}A + B + (-i\omega)\sigma(\omega)C + (-i\omega)^2\sigma(\omega)D + (-i\omega)^2\sigma(\omega)^2E + (-i\omega)^2F\right)v_0 = 0,
$$

with $v_0 := \begin{pmatrix}\hat{p}\\ u\end{pmatrix}$. We define the help functions

$$
v_1 := (-i\omega)^2v_0,\quad v_2 := \frac{1}{\sigma(\omega)}v_0,\quad v_3 := \sigma(\omega)(-i\omega)v_0,\quad v_4 := \sigma(\omega)^2(-i\omega)v_0. \tag{5.2}
$$

Depending on the choice of $\sigma(\omega)$, we have to add more variables to linearize the equations (5.2). We can now easily insert the vertical, diagonal and convolutional scaling functions for $\sigma(\omega)$. The next step is to transform the system into the time domain. The resulting first order system can now be solved using the implicit Euler method from Chapter 3.4.

Example: Using the convolutional scaling function $\sigma_3(\omega) = \frac{\alpha_2+\frac{\alpha_3}{-i\omega}}{\beta_1-\beta_2 i\omega}$ for the problem above

yields the system:

$$\begin{aligned} Bv_0 + Fv_1 + Av_2 + Cv_3 + Dv_3' + Ev_4' &= 0, \\ -v_1 + v_0' &= 0, \\ -\beta_2 v_0 + \alpha_2 v_2 - \beta_1 v_1 &= 0, \\ \alpha_2 v_1 - \beta_2 v_3 + v_6 - \beta_1 v_4' &= 0, \\ \alpha_3 v_2 - v_5' &= 0, \\ \alpha_3 v_1 - v_6' &= 0, \\ \alpha_3 v_3 - v_7' &= 0, \end{aligned}$$

corresponding to the example in Section 3.4.

5.1 Example 1

In this example we want to show a two-dimensional waveguide using the convolutional complex scaling. Figure 5.2 shows the wave diffusion in the waveguide, which is highlighted in the first plot. We use infinite elements for the exterior domain. The geometry is the same for all following examples. Corresponding to Figure 5.1 we have set the wave speed inside the waveguide as $c_0 = 1$ and outside as $c_1 = \sqrt{1/60}$. In all examples we set a time dependent source $f(t) = 15\cos(5t)$ in the left corner.

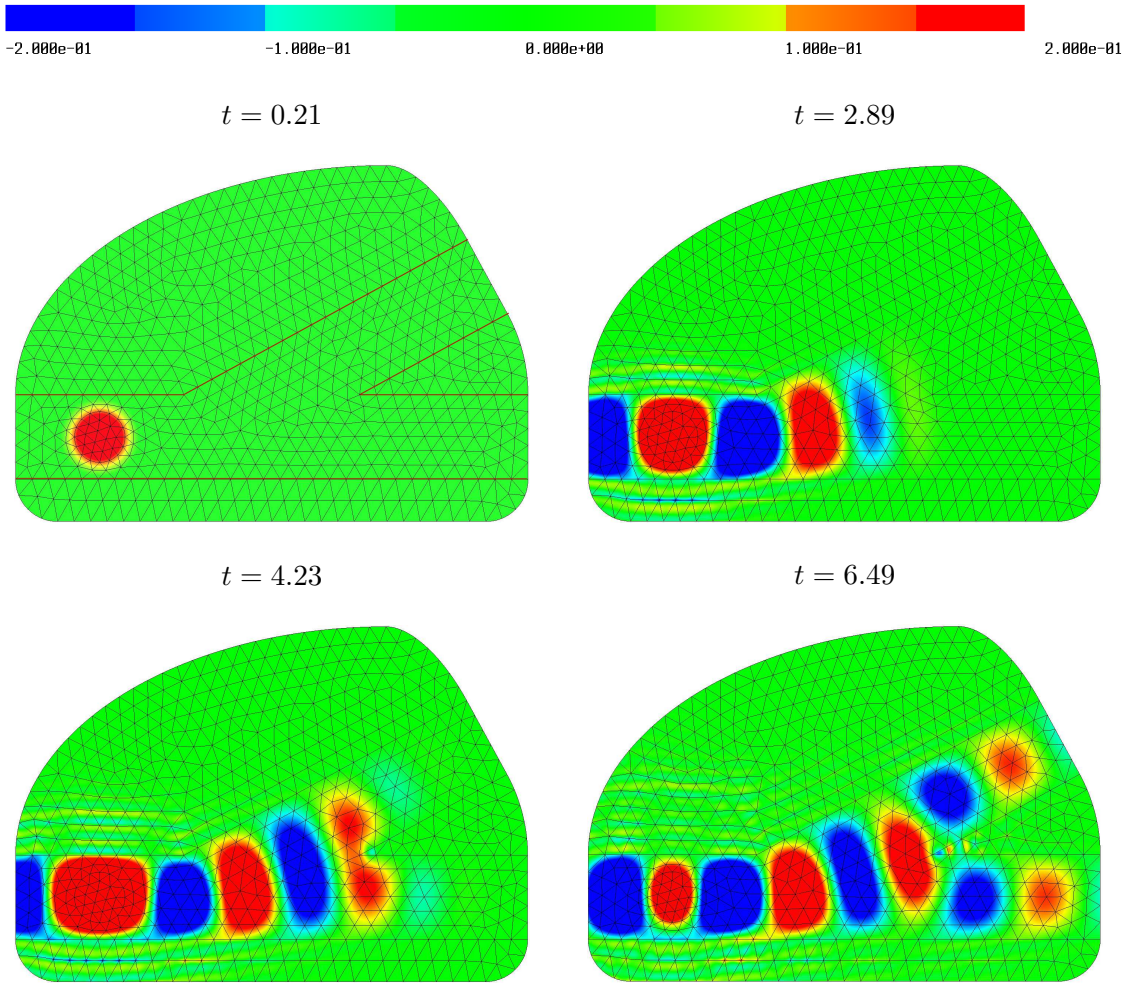

Figure 5.2: Waveguide with time dependent source and $c_1 = \sqrt{1/60}$.

The energy propagates along the waveguide and most of it flows out of it, such that no energy reflects back from the outside. We observe that, as we have set different wave speeds c_0 and c_1, the wave propagation is much slower outside of the wave guide.

5.2 Example 2

As a second example we take the problem from above, but set the outer wave speed as $c_1 = \sqrt{1/10}$. We see in Figure 5.4 that the wave speed outside of the waveguide is higher compared to the first example.

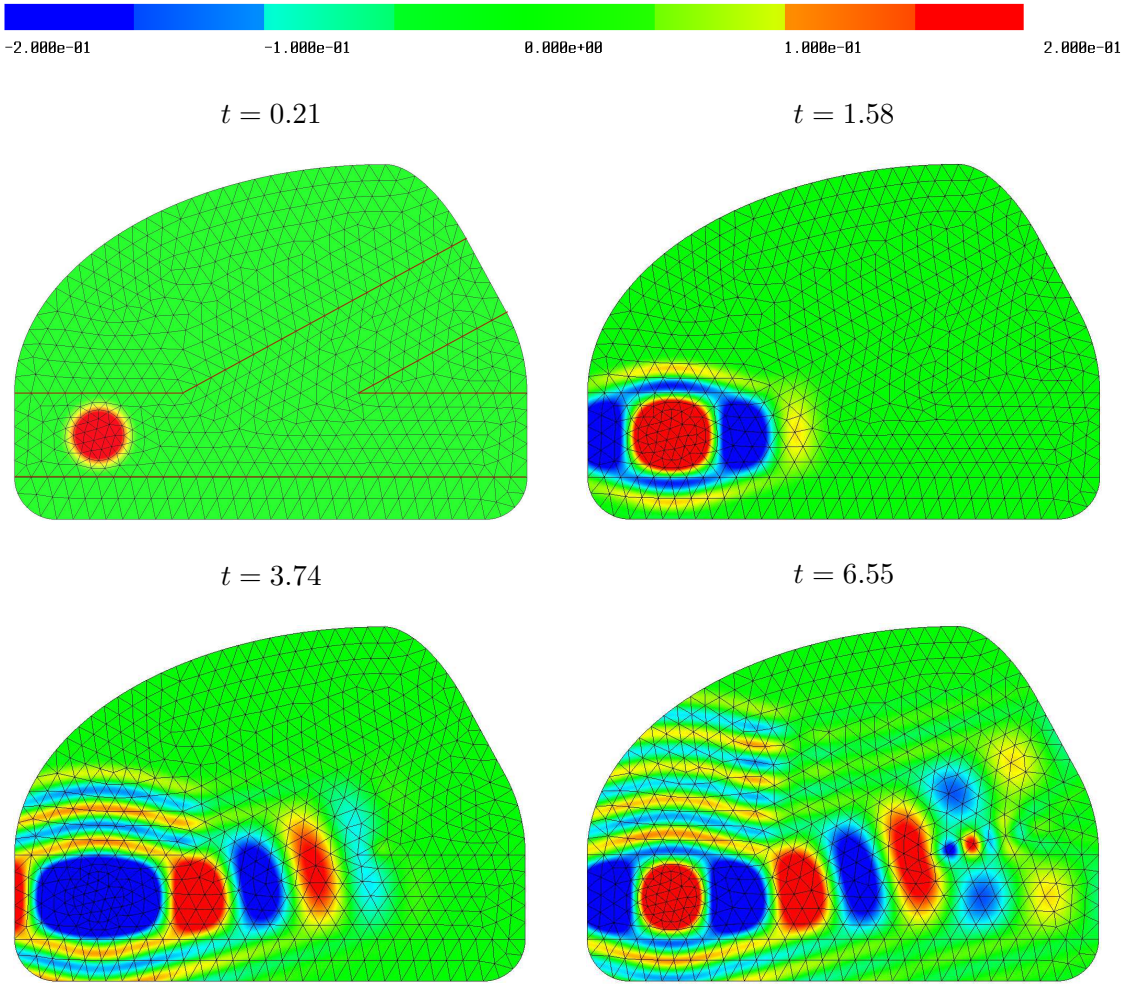

Figure 5.3: Waveguide with time dependent source with outer wave speed $c_1 = \sqrt{1/10}$.

As the wave speed outside of the waveguide is now higher than in the first example, less energy is directed along the waveguide. Again, the solution is well damped at the boundary.

5.3 Example 3

In Chapter 4 we have argued that the vertical scaling fails to damp the solution of the Klein-Gordon problem, which is related to two-dimensional wave guides. To this end, we apply the vertical scaling $\sigma_1(\omega)$ to the problem of the previous example, again setting $c_1 = \sqrt{1/10}$.

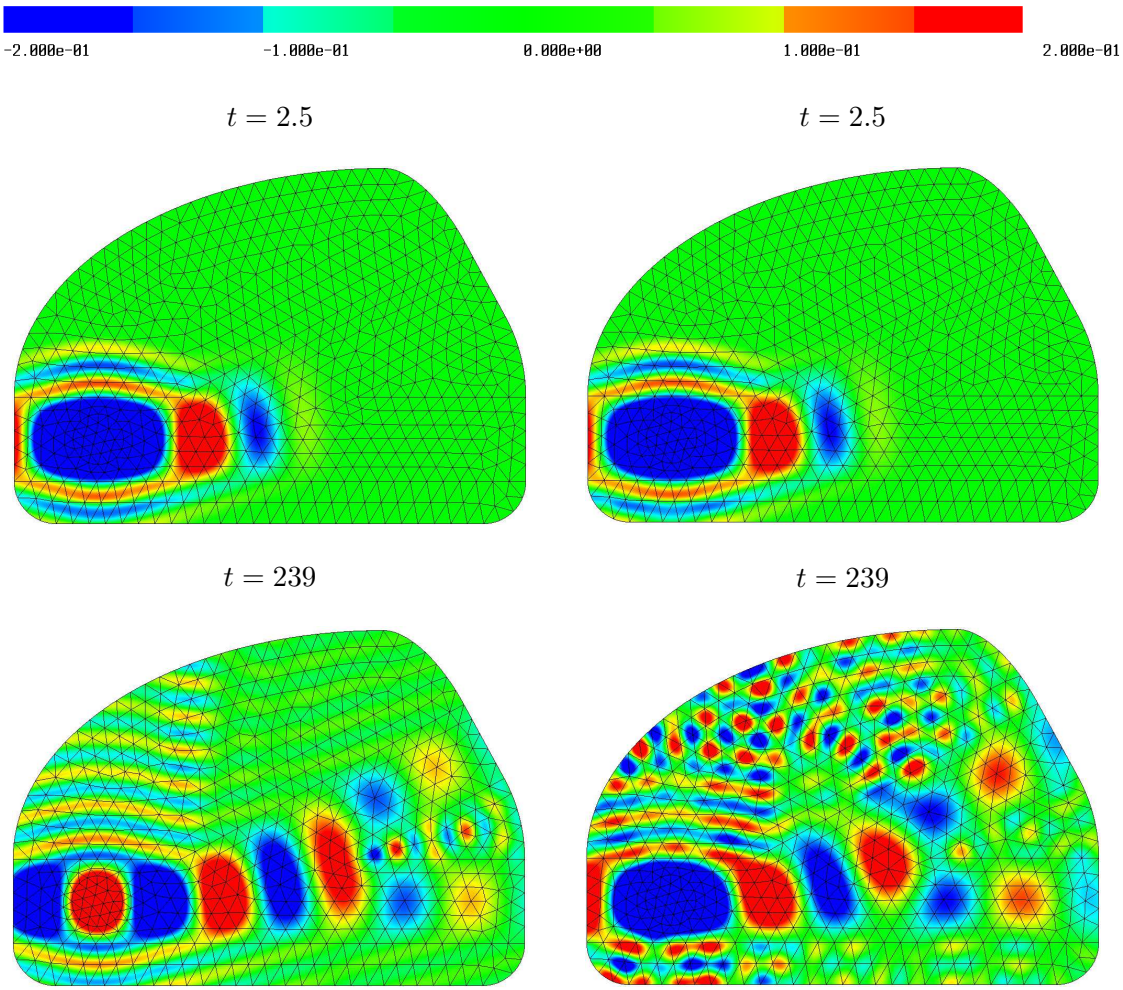

Figure 5.4: Waveguide with time dependent source with convolutional scaling $\sigma_3(\omega)$ on the left and vertical scaling $\sigma_1(\omega)$ on the right.

The solutions are the same at first, but the vertical scaling fails to damp the solution at the boundary, and energy is reflected back. Comparing the two solutions for $t = 239$ we observe that the solution inside the wave guide is distorted when using the vertical scaling.

6 Computational Costs

We mention again that problems were implemented using the finite element software *Netgen/NGSolve*. We have used different time discretization methods for the one- and two-dimensional problems and further examine the difference in their computational costs. We used shared memory parallelization with 12 kernels for all computations on a computer with four Intel Xeon CPU E7-8867 v3 with 16x2.50GHz and 2048GiB memory.

6.1 Time integration without Schur complement

To compare the computational costs for the different scaling functions we consider a one-dimensional Helmholtz problem on $\Omega_{\text{int}} = [-20, 20]$ and PMLs $[-60, -20], [20, 60]$ with time step size $\tau = 0.001$ and no right-hand side. Figure 6.1 shows the average duration of one time step for computing the solution over the mesh size with finite element order 2. In this example we used the second order time integration method without Schur complement inversion from Chapter 3.5.

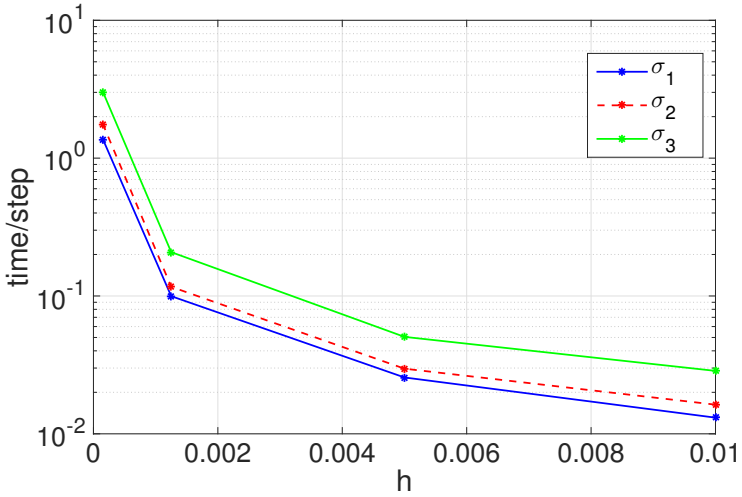

Figure 6.1: The average duration of one time step over mesh size h.

The computational time is the largest for the convolutional scaling σ_3 (light green) as it needs three additional help functions compared to the diagonal scaling σ_2 (red dashed), which needs two, and the vertical scaling σ_1 (blue) needing none. For this example, where all three scaling functions damp the solution well, the vertical scaling is naturally the best choice as it is the cheapest, but we have shown in earlier examples that for the Klein-Gordon

problem it does not manage to damp the solution and can therefore not be used. In Example (4.6.3) we showed that, using the convolutional scaling, the mesh size h of the outer domain can be chosen much larger than for the diagonal scaling, and the computational costs can thus be reduced. For all scalings, the largest amount of the time is taken up by calculation and application of the matrix factorization.

6.2 Time integration with Schur complement

To compare the two time integration methods we consider the same problem as for the second order time integration without Schur complement inversion from above with the linearization method from Chapter 3.4 with Schur complement inversion. Using the convolutional scaling with the second order time integration yields a more expensive computation due to the use of more additional help functions enlarging the system matrix. But since it is the scaling we most likely want to use, we want to compare its performance with the second order method to the linearization method. Figure 6.2 shows the average duration of one time step for the second order method (light green) and the linearization method (blue). Comparing this to Figure 6.1 we see that the computational time of the linearization method is even smaller than the computational time for the vertical scaling $\sigma_1(\omega)$ with the second order scheme. Note that, within the linearization method, the matrix to be inverted has the same size for all scaling functions.

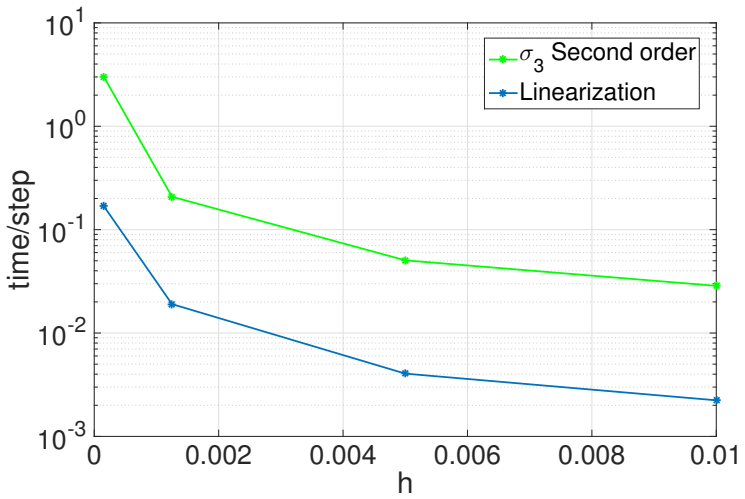

Figure 6.2: The average duration of one time step over mesh size h with the second order method (light green) and the linearization method (blue).

7 Conclusion

In this thesis we considered the complex scaling method for the wave equation and the Klein-Gordon equation. The problems are transformed via the Fourier transformation, and a complex coordinate stretching is applied to the coordinate of the direction of radiation. This was done in cartesian, radial and curvilinear coordinates in Chapter 2. Though the complexity of notation may increase with curvilinear coordinates, we can now use the PML method on various shapes of the domain of interest. We compared the effect of different complex scalings, the vertical, diagonal and convolutional scaling, on the outgoing solutions. For the Helmholtz problem in one dimension we have found that all scalings damp the solution, but the solution of the Klein-Gordon problem can only be damped with the diagonal and convolutional scaling, whereas the diagonal scaling may produce oscillations. The vertical scaling proves to have undesired influences on the exponential decay of the solutions, as was shown for the one-dimensional case in Chapter 4. As the one-dimensional Klein-Gordon equation is related to wave guides in more dimensions, we have found that the convolutional scaling is also preferable for two-dimensional wave guides, and that the vertical scaling fails to damp the solution.

We have provided numerical examples in one and two dimensions to show the behavior of the solutions for different scalings. The time discretization was done with two different methods, a second order time integration and a linearization method, which has smaller computational costs.

8 Literature

[Ber94] Bérenger, Jean-Pierre: *A perfectly matched layer for the absorption of electromagnetic waves.* Journal of Computational Physics, 114(2):185-200, 1994.

[Bob06] Bobenko, Alexander: *Differentialgeometrie von Kurven und Flächen.* Technische Universität Berlin, 2006.

[Cia78] Ciarlet, Philippe G.: *The finite element method for elliptic problems.* Amsterdam : North-Holland Publishing Co. - xix+530 S. - Studies in Mathematics and its Applications, Vol. 4, 1978.

[Giv04] Givoli, Dan: *High-order local non-reflecting boundary conditions: a review.* Wave Motion, 39(4):319-326, 2004.

[HL09] Hohage, Thorsten, Nannen, Lothar: *Hardy space infinite elements for scattering and resonance problems.*, SIAM J. Numer. Anal. 47, pp. 972 996. 2009.

[Jue15] Juengel, Ansgar: *P*artielle Differentialgleichungen. Technische Universität Wien, 2015.

[KKS12] Kaltenbacher, Barbara; Kaltenbacher, Manfred; Sim, Imbo: *A modified and stable version of a perfectly matched layer technique for the 3-d second order wave equation in time domain with an application to aeroacoustics.* Institute of Mechanics and Mechatronics. Technische Universität Wien, 2012.

[Nan08] Nannen, Lothar. *Hardy-Raum Methoden zur numerischen Lösung von Streu- und Resonanzproblemen auf unbeschränkten Gebieten.* Universität Göttingen, 2008.

[Nan16] Nannen, Lothar: *Streu- und Resonanzprobleme.* Technische Universität Wien, 2016.

[Nat13] Nataf, Frédéric: *Absorbing boundary conditions and perfectly matched layers in wave propagation problems. Direct and Inverse problems in Wave Propagation and Applications.* 14, de Gruyter, pp.219-231,Radon Ser. Comput. Appl. Math., 2013.

[NW19] Nannen, Lothar; Wess, Markus: *Complex scaled infinite elements for exterior Helmholtz problems.* arXiv: 907.09746 (2019).

[PS10] Pasciak, Joseph E.; Seungil, Kim: *Analysis of a Cartesian PML approximation to acoustic scatteringproblems in* $\mathbb{R}^2$. J. Math. Anal. Appl., 370 (2010) 168-186, 2010.

[Sch97] Schöberl, Joachim: *NETGEN, An advancing front 2D/3D-mesh generator based on abstract rules.* Computing and Visualization in Science 1, Nr. 1, S. 41-52, 1997.

[Sch14] Schöberl, Joachim: *C++11 Implementation of Finite Elements in NG-Solve.* Institute for Analysis and Scientific Computing, Technische Universität Wien, 2014.

[Sch18] Schöberl, Joachim: *Numerical Methods for Partial Differential Equations.* Technische Universität Wien, 2018.